1991-12

Performance analysis of non-coplanar synergetic maneuvers

Spriesterbach, Thomas P.

Monterey, California. Naval Postgraduate School

NAVAL POSTGRADUATE SCHOOL
Monterey, California

THESIS

Performance Analysis of Non-Coplanar Synergetic Maneuvers

by

Thomas P. Spriesterbach

December 1991

Thesis Advisor I. M. Ross

REPORT DOCUMENTATION PAGE

1a. REPORT SECURITY CLASSIFICATION Unclassified		1b. RESTRICTIVE MARKINGS	
2a. SECURITY CLASSIFICATION AUTHORITY		3. DISTRIBUTION/ AVAILABILITY OF REPORT Approved for public release; distribution is unlimited.	
2b. DCLASSIFICATION/DOWNGRADING SCHEDULE			
4. PERFORMING ORGANIZATION REPORT NUMBER(S)		5. MONITORING ORGANIZATION REPORT NUMBER(S)	
6a. NAME OF PERFORMING ORGANIZATION Naval Postgraduate School	6b. OFFICE SYMBOL *(If Applicable)*	7a. NAME OF MONITORING ORGANIZATION Naval Postgraduate School	
6c. ADDRESS *(city, state, and ZIP code)* Monterey, CA 93943-5000		7b. ADDRESS *(city, state, and ZIP code)* Monterey, CA 93943-5000	
8a. NAME OF FUNDING/SPONSORING ORGANIZATION	6b. OFFICE SYMBOL *(If Applicable)*	9. PROCUREMENT INSTRUMENT IDENTIFICATION NUMBER	
8c. ADDRESS *(city, state, and ZIP code)*		10. SOURCE OF FUNDING NUMBERS	
		PROGRAM ELEMENT NO.	PROJECT NO.
			TASK NO.
			WORK UNIT ACCESSION NO.

11. TITLE *(Include Security Classification)*
Performance Analysis of Non-Coplanar Synergetic Maneuvers

12. PERSONAL AUTHOR(S)
Spriesterbach, Thomas P..

13a. TYPE OF REPORT	13b. TIME COVERED	14. DATE OF REPORT *(year, month,day)*	15. PAGE COUNT
Master's Thesis	FROM TO	Decembr 1991	94

16. SUPPLEMENTARY NOTATION
The views expressed in this thesis are those of the author and do not reflect the official policy or position of the Department of Defense or the U.S. Government.

17. COSATI CODES			18. SUBJECT TERMS *(continue on reverse if necessary and identify by block number)*
FIELD	GROUP	SUBGROUP	Synergetic, Aerocruise, Aerobang, Hypervelocity

19. ABSTRACT *(Continue on reverse if necessary and identify by block number)*

Maneuvers employing atmospheric forces to assist in orbital changes hold potential for significant fuel savings over purely exoatmospheric propulsive methods. The term synergetic has been coined to describe the combination of propulsive and atmospheric forces used by a maneuvering flight vehicle. This thesis concentrates on non-coplanar synergetic maneuvers using two different control methods for various lifting bodies over a range of heating rates and orbital speeds. The objective of this thesis is to study the aerocruise and aerobang maneuvers. The aerocruise maneuver has been studied for more than twenty years and is commonly thought to be the fuel-optimal solution to a maneuver flown at a constant heating rate. A new maneuver, the aerobang, has recently laid doubt as to the optimality of the aerocruise maneuver. The aerobang maneuver demonstrates the ability to yield a higher inclination change for a given amount of fuel as compared to the aerocruise maneuver. Within this thesis a computer code is developed to model both the aerobang and aerocruise maneuvers. It is shown that there exist flight regimes where the aerobang method is superior to the aerocruise method.

20. DISTRIBUTION/AVAILABILITY OF ABSTRACT	21. ABSTRACT SECURITY CLASSIFICATION	
[X] UNCLASSIFIED/UNLIMITED [ ] SAME AS RPT. [ ] DTIC USERS	Unclassified	
22a. NAME OF RESPONSIBLE INDIVIDUAL I. M. Ross	22b. TELEPHONE (Include Area Code) (408) 646-2772	22c. OFFICE SYMBOL AA/Ro

DD FORM 1473, 84 MAR 83 APR edition may be used until exhausted SECURITY CLASSIFICATION OF THIS PAGE

All other editions are obsolete Unclassified

Approved for public release; distribution is unlimited.

Performance Analysis of Non-Coplanar Synergetic Maneuvers

by

Thomas P. Spriesterbach
Lieutenant , United States Navy
B.S., United States Naval Academy, 1983

Submitted in partial fulfillment of the requirements for the degree of

MASTER OF SCIENCE IN ASTRONAUTICAL ENGINEERING

from the

NAVAL POSTGRADUATE SCHOOL
December 1991

ABSTRACT

Maneuvers employing atmospheric forces to assist in orbital changes hold potential for significant fuel savings over purely exoatmospheric propulsive methods. The term synergetic has been coined to describe the combination of propulsive and atmospheric forces used by a maneuvering flight vehicle. This thesis concentrates on non-coplanar synergetic maneuvers using two different control methods for various lifting bodies over a range of heating rates and orbital speeds. The objective of this thesis is to study the aerocruise and aerobang maneuvers. The aerocruise maneuver has been studied for more than twenty years and is commonly thought to be the fuel-optimal solution to a maneuver flown at a constant heating rate. A new maneuver, the aerobang, has recently laid doubt as to the optimality of the aerocruise maneuver. The aerobang maneuver demonstrates the ability to yield a higher inclination change for a given amount of fuel as compared to the aerocruise maneuver. Within this thesis a computer code is developed to model both the aerobang and aerocruise maneuvers. It is shown that there exist flight regimes where the aerobang method is superior to the aerocruise method.

TABLE OF CONTENTS

I. INTRODUCTION 1
A. THESIS SCOPE 2
B. BACKGROUND 3
1. Aeroglide 4
2. Aerocruise 5
3. Aerobang 7
II. FLIGHT VEHICLES 8
A. ENTRY RESEARCH VEHICLE 8
B. MANEUVERABLE REENTRY RESEARCH VEHICLE 11
III. EQUATIONS OF MOTION 15
A. DERIVATION OF EQUATIONS 16
B. DERIVATION OF THE INCLINATION 23
IV. CONTROL LAWS 25
A. AEROCRUISE CONTROL LAW 25
B. AEROBANG CONTROL LAW 27
1. Mechanics of Convergence 29
2. Newton's Method of Convergence 30
3. Initial Guess of Angle of Attack 31
V. PROGRAM DEVELOPMENT 32
A. MAIN PROGRAM 32
B. SUBROUTINES 34
1. Subroutine CNTRL 34
a. Aerobang Control Model 36

b. Aerocruise Control Model 36
2. Subroutine ACEL 37
3. Subroutine ORB 37
4. Subroutines HDR and WRT 37
5. Subroutine RK4 38
C. PROGRAM USAGE 38
D. PROGRAM VALIDATION 40
VI. ANALYSIS 42
A. FORMULATION OF THE SOLUTION 42
B. SUPERCIRCULAR PROFILES 44
1. High Heating Rate 44
a. ERV 44
b. MRRV 46
2. Low Heating Rate 47
a. ERV 47
b. MRRV 48
C. SUBCIRCULAR PROFILES 49
1. High Heating Rate 49
a. ERV 49
b. MRRV 52
2. Low Heating Rate 54
a. ERV 54
b. MRRV 57
D. MASS FRACTION EFFECTS 59
VII. CONCLUSIONS AND RECOMMENDATIONS 62

1. CONCLUSIONS 62
2. FOLLOW ON TOPICS 65
APPENDIX A PROGRAM ORBIT 67
SAMPLE INPUT DATA FILE "DATA.DAT" 76
SAMPLE INPUT FILE "AERO.DAT" 77
SAMPLE OUTPUT FILE "OUT.DAT" 78
LIST OF REFERENCES 79
INITIAL DISTRIBUTION LIST 81

LIST OF FIGURES

Figure 1. Orbital Transfer Maneuver 2
Figure 2. Heating Rate Curve 6
Figure 3. Graphical Representation of Aerocruise Maneuver 7
Figure 4. Three-view Diagram of ERV 9
Figure 5. Coefficient of Lift vs Angle of Attack for ERV 10
Figure 6. Coefficient of Drag vs Angle of Attack for ERV 10
Figure 7. CL/CD vs Angle of Attack for ERV 11
Figure 8. Three-view Diagram of MRRV 12
Figure 9. Coefficient of Lift vs Angle of Attack for MRRV 13
Figure 10. Coefficient of Drag vs Angle of Attack for MRRV 13
Figure 11. CL/CD vs Angle of Attack for MRRV 14
Figure 12. Graphical Representation of Variables 15
Figure 13. Spacecraft Forces During Atmospheric Interaction 20
Figure 14. Graphical Example of Angle of Attack Solution 29
Figure 15. Flow Chart for Main Program 33
Figure 16. Flow Chart of CNTRL Subroutine 35
Figure 17. Inclination Change for ERV k=.94 44
Figure 18. Angle of Attack vs Mass Fraction ERV k=.94 44
Figure 19. Inclination Change for ERV k=.95 44
Figure 20. Angle of Attack vs Mass Fraction for ERV k=.95 44
Figure 21. Inclination Change for MRRV k=.99 47
Figure 22. Inclination Change for MRRV k=.985 47
Figure 23. Inclination Change for MRRV k=.98 47

Figure 24. Fuel Percent Difference over Aerocruise vs k Factor for ERV (High Heating Rate) 51
Figure 25. ERV k=1.1 Angle of Attack Profile unaugmented 52
Figure 26. ERV k=1.1 Angle of Attack Profile AOB augmented 52
Figure 27. Fuel Percentage Difference over Aerocruise vs k Factor for MRRV (High Heating Rate) 54
Figure 28. Fuel Percentage Difference over Aerocruise vs k Factor for ERV (Low Heating Rate) 56
Figure 29. Fuel Percentage Difference over Aerocruise vs k Factor for MRRV (Low Heating Rate) 58
Figure 30. Fuel Percentage Difference over Aerocruise vs Mass Fraction Fuel Expended for ERV (k=1.03) 61
Figure 31. Efficiency Regions for the ERV 62
Figure 32. Efficiency Regions for the MRRV 63

LIST OF TABLES

TABLE 1. INPUT FILE AERO.DAT 39
TABLE 2. INPUT FILE DATA.DAT 40
TABLE 3. ORBITAL DYNAMIC VALIDATION 41
TABLE 4. PROGRAM VALIDATION 41
TABLE 5. SUMMARY OF ERV FLIGHT PROFILES FOR HIGH HEATING RATE 50
TABLE 6. SUMMARY OF MRRV FLIGHT PROFILES FOR HIGH HEATING RATE 53
TABLE 7. SUMMARY OF ERV FLIGHT PROFILES FOR LOW HEATING RATE 55
TABLE 8. SUMMARY OF MRRV FLIGHT PROFILES FOR LOW HEATING RATE 57
TABLE 9. EFFECT OF MASS FRACTION ON INCLINATION CHANGE EFFICIENCY 60

LIST OF VARIABLES

a	Acceleration of the flight vehicle.
A_R	Flight vehicle acceleration in the radial direction.
A_S	Flight vehicle acceleration in the tangential direction.
A_W	Flight vehicle acceleration in the binormal direction.
C_D	Coefficient of drag on flight vehicle.
C_L	Coefficient of lift on flight vehicle.
C_1	Zeroth order coefficient of binomial expansion of C_L vs angle of attack.
C_2	First order coefficient of binomial expansion of C_L vs angle of attack.
C_3	Second order coefficient of binomial expansion of C_L vs angle of attack.
C_4	Zeroth order coefficient of binomial expansion of C_D vs angle of attack.
C_5	First order coefficient of binomial expansion of C_D vs angle of attack.
C_6	Second order coefficient of binomial expansion of C_D vs angle of attack.
D	Drag on flight vehicle.
F	Sum of all forces on flight vehicle composed of the components $F_{x'}$, $F_{y'}$, and $F_{z'}$.
$F_{x'}$	Forces acting on the flight vehicle along the x axis in flight vehicle frame of reference.

$F_{y'}$	Forces acting on the flight vehicle along the y axis in flight vehicle frame of reference.
$F_{z'}$	Forces acting on the flight vehicle along the z axis in flight vehicle frame of reference.
g	Local gravity.
h	Angular momentum of the flight vehicle.
i	Orbit inclination.
ISP	Specific Impulse
$\vec{k}$	Unit vector along Z axis of the inertial coordinate system
k	Coefficient for heating rate formula.
L	Lift on flight vehicle.
m_a	Mass of the flight vehicle.
m	Power coefficient for velocity in the heating rate formula.
n	Power coefficient for density in the heating rate formula.
$\dot{Q}$	Stagnation point heating rate of flight vehicle.
$\dot{Q}_o$	Reference stagnation point heating rate of flight vehicle.
r	Geocentric radius of flight vehicle.
r_o	Reference geocentric radius of flight vehicle.
r_s	Reference geocentric radius for atmospheric model.
S	Reference area of flight vehicle.
T	Thrust of flight vehicle.
V	Speed of flight vehicle.
W	Weight of flight vehicle, based on local gravity and mass.
X,Y,Z	Cartesian coordinates for inertial reference frame.
x,y,z	Cartesian coordinates for rotating reference frame.
x',y',z'	Cartesian coordinates for flight vehicle reference frame.

α	Angle of Attack of flight vehicle.
β	Coefficient for scale height in atmospheric model.
ψ	Heading of flight vehicle based on angle from equatorial plane.
ϕ	Declination of spacecraft.
γ	Flight path angle, referenced to local horizon.
θ	Right ascension of spacecraft.
Ω	Angular velocity of the flight vehicle.
ρ	Density of the atmosphere.
ρ_o	Reference density of the atmosphere.
ρ_s	Reference density of the atmosphere for atmospheric model.
σ	Angle of bank of flight vehicle.

I. INTRODUCTION

The concept of maneuvering within the atmosphere by flight vehicles moving at orbital or near orbital speeds dates back to Sanger's idea of a suborbital spacecraft using aerodynamic lift to extend its range [Ref. 1]. While the idea is not new, the practical application, using lifting bodies at hypervelocities, may be within reach. New materials, propulsion, and engineering techniques have revived the idea of a synergetic maneuver. The term synergetic has been coined to describe the maneuvering of a spacecraft within the atmosphere using the combination of propulsive and aerodynamic forces. A maneuver using atmospheric forces to assist in orbital changes holds the potential for significant fuel savings over a purely exoatmospheric propulsive method [Ref. 2]. Mission applications of these types of maneuvers have been identified in three contexts; 1) synergetic plane change, 2) planetary missions, and 3) high earth orbit to low earth orbit rendezvous [Ref. 3: p. 3]. These three categories encompass the totality of useful application of this type of maneuver. This thesis is concerned with category one, the synergetic plane change. This application deals with non-coplanar orbital transfers, the interest of which is limited to the inclination change. A typical flight profile of a spacecraft executing a maneuver of this nature would require a deorbit burn which would put the spacecraft into a trajectory grazing the atmosphere, an aerodynamic turn, and finally a circularization maneuver at the desired altitude (Figure 1).

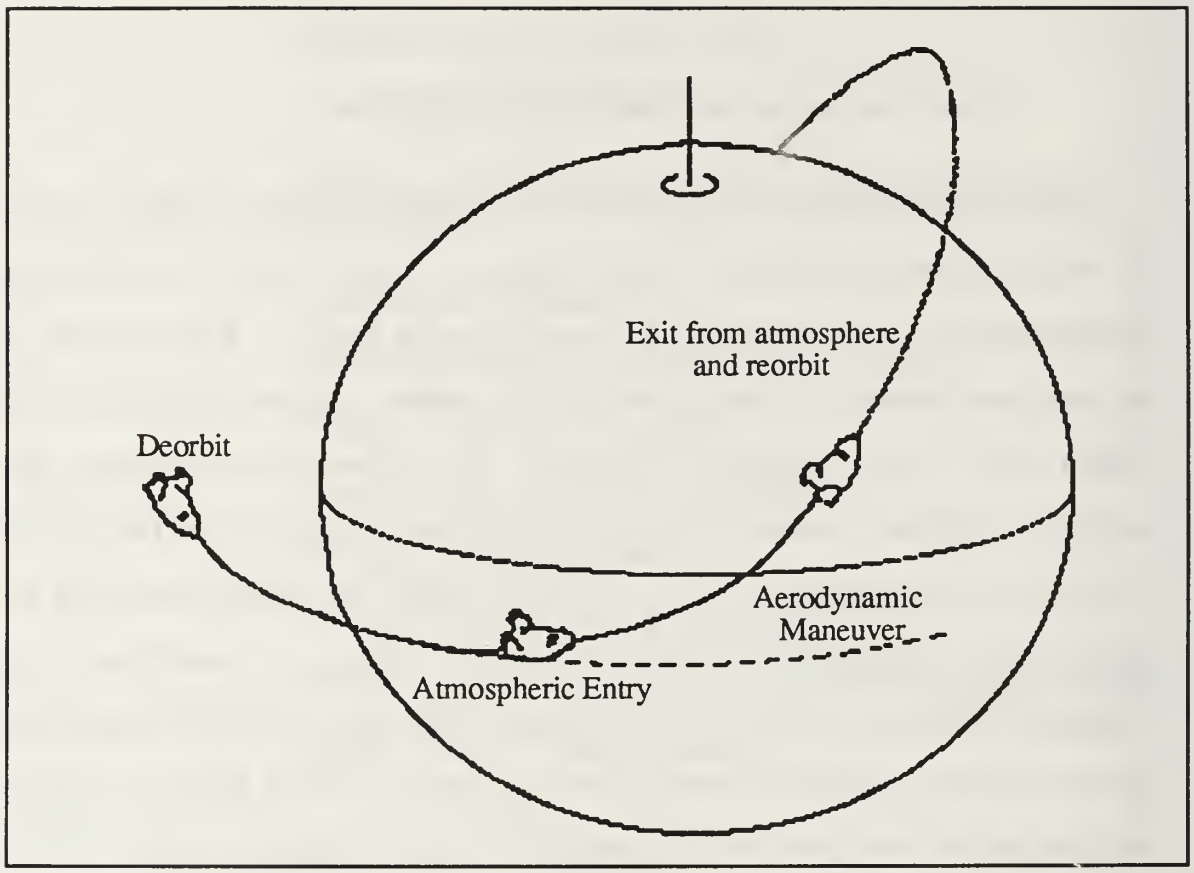

Figure 1. Orbital Transfer Maneuver

A. THESIS SCOPE

In the search for the optimum synergetic maneuver, three methods have been studied: the aeroglide, the aerocruise, and the aerobang. The aeroglide maneuver uses no propulsive force during the atmospheric interaction, theoretically giving this method an infinite inclination change per kilogram of fuel used. The penalty for the aeroglide maneuver is the extremely high heating rates caused by the dense atmosphere from the required low altitudes. The aerocruise maneuver was developed to overcome the heating rate problem created by the aeroglide method. In order to maintain a constant heating rate the aerocruise maneuver uses a combination of propulsion and aerodynamics to

achieve an inclination change. For more than twenty years, this method has been studied to determine the optimal regimes of operation for this maneuver. A recent study has raised doubt to the optimality of the aerocruise maneuver and proposed another maneuver based on a maximum throttle setting and a modulation of the angle of attack [Ref. 3]. This new aerobang maneuver demonstrates the ability to yield a higher inclination change per kilogram of fuel used when compared to the aerocruise maneuver under like conditions.

This thesis analyzes two control methods of synergetic maneuvers, the aerocruise and the aerobang method. Each of the two maneuvers have similar goals of maintaining a constant heating rate while executing the aerodynamic turn. An evaluation, analysis, and comparison of the two maneuvers over a range of maximum lift to drag ratios ($(L/D)_{max}$) and heating rates will shed light on the capabilities and inadequacies of each control method. The analysis is limited to the actual maneuver itself at the necessary altitude required for its execution. It was assumed that the the method of entry or exit from the atmosphere for the two maneuvers would be identical and would not be a factor in the overall efficiency of the maneuver.

The study includes a program developed specifically to model the aerocruise and aerobang control laws. The performance of each of these strategies are analyzed over a variety of orbital speeds and altitudes. The intent is to develop insight into the range of capabilities for each method and conditions under which aerobang might be more efficient than aerocruise.

B. BACKGROUND

Synergetic non-coplanar orbital transfers utilize a portion or all of the lift generated by the body in a direction perpendicular to the orbital plane. A force

applied in this direction will cause a change in the inclination of the orbit. The effect of the force on the inclination is maximized at the ascending and descending nodes of the orbits but has no effect at the apex of the orbit (i.e. 90 degrees from the nodal crossing). This maximizing effect at the node necessitates that the maneuver be completed within a short time span relative to the orbital period of the flight vehicle. Three methods of inclination change have been proposed so far: aeroglide, aerocruise, and aerobang. While this thesis deals with only two of these, the third method, aeroglide, would be of use in bringing the spacecraft to the appropriate position in which to commence the maneuver.

1. Aeroglide

During a non-coplanar transfer the aeroglide maneuver seeks to change the orbital inclination of the spacecraft. The maneuver consists of three parts, the deorbit, the aerodynamic turn, and the reorbit. The first and last segments of the maneuver are purely propulsive and generic to any of the three methods discussed within this thesis. To describe the aerodynamic turn of the aeroglide maneuver, it must be understood that no propulsive forces are used within the atmosphere. In order to maximize the plane change, the maneuver is most efficient at an angle of attack that produces the maximum lift-to-drag ratio. The lifting body is oriented with the generated lift vector normal to the spacecraft's orbit. To generate the necessary lift for an effective plane change, the vehicle is flown at an orbital speed and a low altitude where the atmosphere is very dense. This flight profile results in an extremely high heating rate for the flight vehicle, possibly beyond the capabilities of the spacecraft. If the heating rate problem can be overcome, the aeroglide maneuver requires fuel expenditures only to

deorbit and reorbit, significantly reducing the fuel required to effect the same plane-change using a pure propulsive method. [Ref. 5: p 104]

The extreme heating rate required by the aeroglide maneuver hinders its use as an effective method for non-coplanar transfers. The heating rate profile of the maneuver begins at a low value as it enters the atmosphere and builds to its highest value at the minimum orbital altitude. A possible use for the aeroglide maneuver would be in conjunction with another synergetic plane change maneuver. A proposed flight profile would be: after the deorbit burn the spacecraft would assume an aeroglide profile until the predetermined altitude, velocity, and heating rate were achieved, then the follow-on maneuver would be executed, and finally an aeroglide maneuver to exit the atmosphere and reboost. Both aeroglide portions of the flight path would not be at the optimum glide profiles for an aeroglide maneuver, but some gain of inclination change would be realized until the selected conditions for the aerocruise or aerobang maneuver are reached.

2. Aerocruise

The aerocruise synergetic maneuver couples the aeroglide maneuver with a propulsive force during the atmospheric interaction. This maneuver is made up of three parts, the deorbit, the aerodynamic turn, and the reorbit, similar to the aeroglide maneuver, the difference being in the method used during the aerodynamic turn. A typical flight profile requires the vehicle to remain on the heating rate boundary; this dictates the aerocruise maneuver to be flown at a specific altitude and speed. Graphically, this profile appears as a point on a speed versus radius graph (Figure 2). This point would just touch the maximum allowable heating rate for the spacecraft. The altitude and speed are

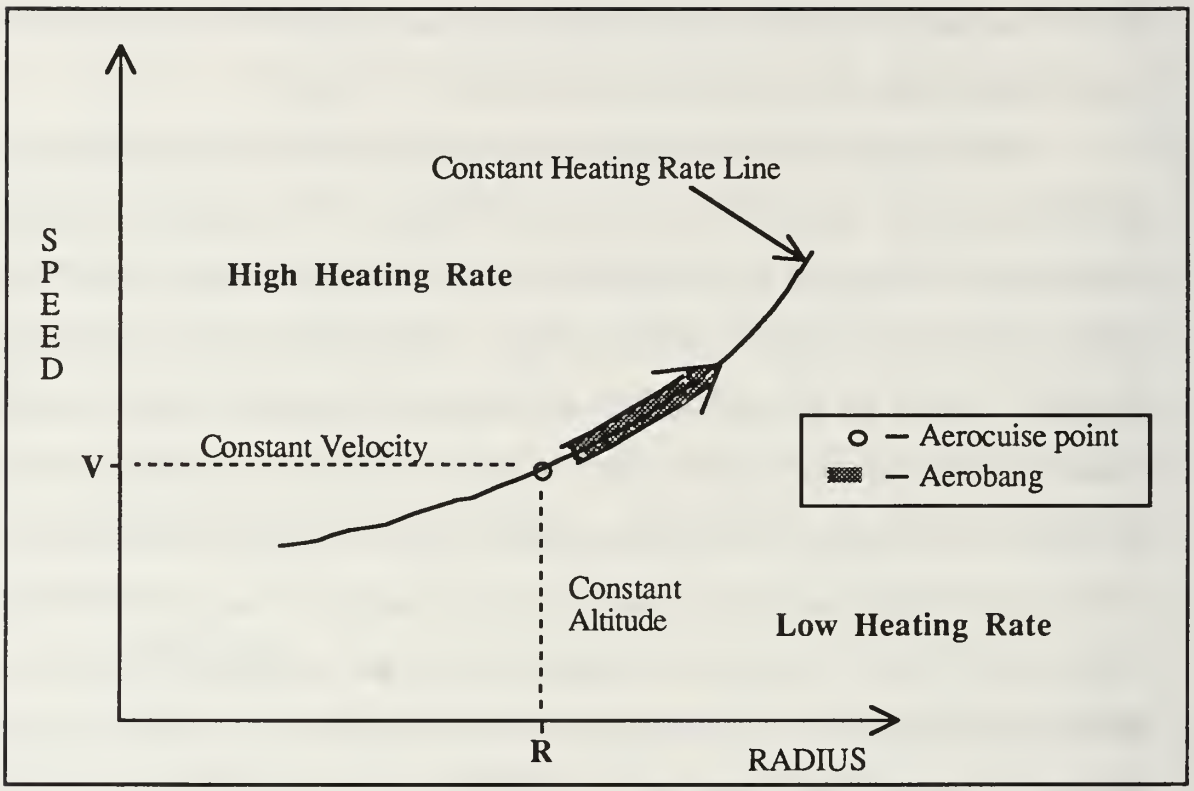

Figure 2. Heating Rate Curve

maintained by a combination of engine throttling and modulation of the flight vehicle angle of bank. The speed is held constant by setting the thrust equal to the drag encountered at the flight altitude. Altitude is maintained by banking the spacecraft to allow for a component of the lift force generated to counteract the apparent centrifugal force (Figure 3). This method allows for a plane-change maneuver without incurring the heating rate problems of the aeroglide maneuver. Conventional wisdom requires that the angle of attack be set at $(L/D)_{max}$ in order to maximize the efficiency of the maneuver [Ref. 3: p. 5]; however, recent studies [Ref. 6: p. 517] have shown that the most efficient (i.e. largest inclination change for a given expenditure of fuel) maneuver is not at $(L/D)_{max}$, but at a lower L/D and a higher angle of attack.

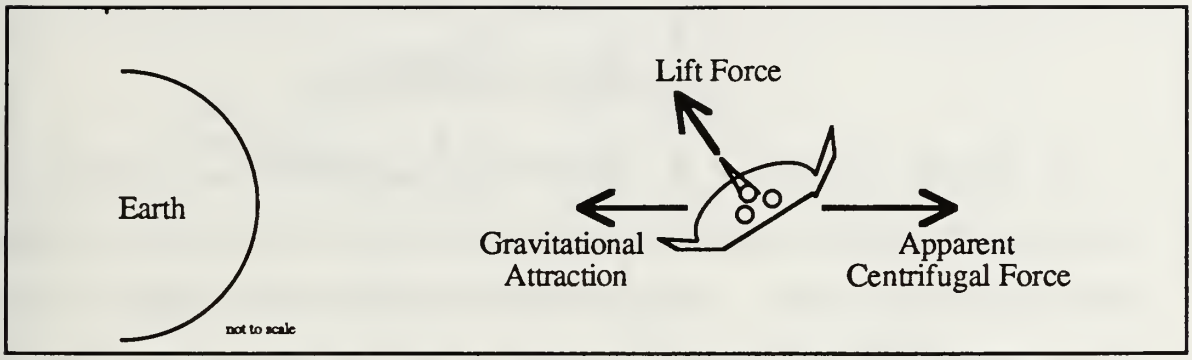

Figure 3. Graphical Representation of Aerocruise Maneuver

3. Aerobang

This method of control is similar to the aerocruise model in that the heating rate of the vehicle is to remain constant, but this is where the similarity ends. The aerobang flight profile allows the vehicle to change its altitude and speed as necessitated by the control law governing the maneuver (Figure 2). As mentioned previously, the most effective use of the lifting force for the orbital plane change is to orient the force normal to the orbital plane; this dictates an angle of bank of 90 degrees for the spacecraft. If the angle of bank is to remain fixed, the only variables left for modulation are the thrust of the vehicle and the angle of attack. The aerobang maneuver modulates the angle of attack and fixes the thrust at the maximum available value. It can be shown that for certain conditions, the aerobang maneuver will achieve a higher inclination change for a given fuel expenditure than the aerocruise maneuver.

II. FLIGHT VEHICLES

To properly understand the similarities and differences between the aerocruise and aerobang maneuvers, a parameter analysis of more than one flight vehicle would be necessary. Ideally, the flight vehicles would be similar in every respect except one, and changes observed on the data output could then be attributed to that differing parameter. Early investigators of synergetic maneuvers came to two main conclusions: first, the lifting body should operate at $(L/D)_{max}$, and second, the L/D should be greater than one to be superior to an all propulsive maneuver [Ref. 3: p. 5]. The emphasis on $(L/D)_{max}$ brought this investigation to select two vehicles for comparison, one which would operate at $(L/D)_{max}$ of approximately 1.8 and the other at 2.6. Flight vehicles which have been designed and have data available provide a sense of reality to the analysis, where as an imaginary flight vehicle and data might skew the study. The two flight vehicles investigated in this thesis are the ERV (Entry Research Vehicle) and the MRRV (Maneuverable Reentry Research Vehicle).

A. ENTRY RESEARCH VEHICLE

The ERV was designed with the idea of investigating and exploiting maneuvers involving long downrange, high crossrange, and synergetic plane changes. The vehicle is 7.62 m long and has a wing span of only 3.96 m, allowing the vehicle to be launched from the cargo bay of the space shuttle. The slenderness ratio of the fuselage is approximately 0.167. Figure 4 shows a three-view sketch of the ERV. Three Marquardt R-40-B rocket motors make up the propulsion system, providing a total of 14679 Newtons of thrust at a specific

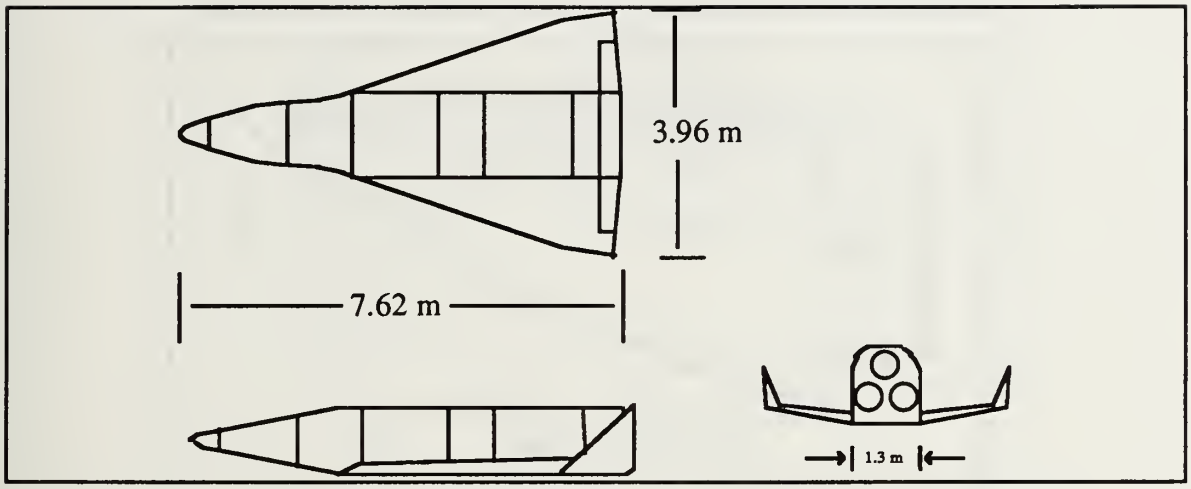

Figure 4. Three-view Diagram of ERV

impulse (ISP) of 295 seconds. Separation weight from the Space Shuttle is planed for 5443 kg with 50% of that made up of fuel.[Ref. 7: pp. 489-90]

For the purpose of modeling within a computer program, the aerodynamic data were approximated by a least squares binomial fit (Figures 5 and 6). Wind-tunnel data for the ERV were obtained from the Martin Marietta Corporation [Ref. 8] and included coefficient of lift and drag data up to Mach 10. These data were used for flight velocities from 8.3 km/sec down to 7.1 km/sec. Although these velocities correspond to Mach numbers of 26 to 22 at the maneuvering altitude, the data from Mach 10 can realistically apply because of the limiting characteristics exhibited by the bow shock and the pressure distribution over the lifting body [Ref. 9: pp. 387-388]. The curve fit was done using a linear statistical model [Ref. 10] and then the coefficients were modified to obtain an L/D vs angle of attack similar to the actual data taken from the wind tunnel tests. From the L/D curve (Figure 7), we see that $(L/D)_{max}$ occurs at approx 10.5 degrees with a value of 1.8.

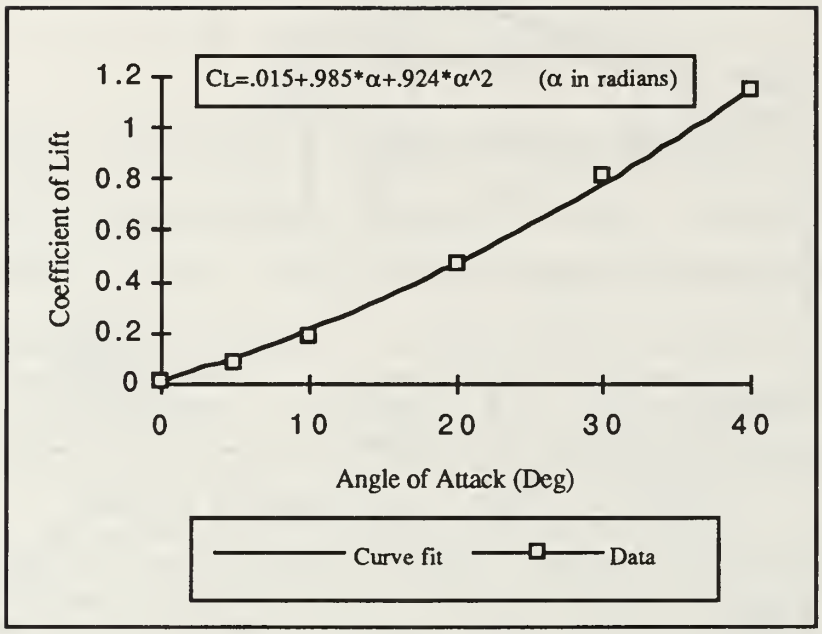

Figure 5. Coefficient of Lift vs Angle of Attack for ERV

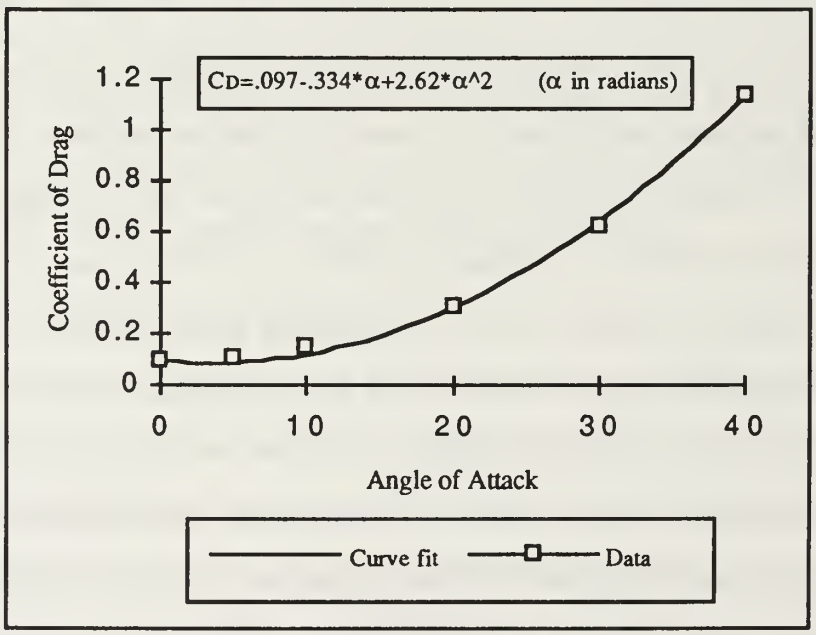

Figure 6. Coefficient of Drag vs Angle of Attack for ERV

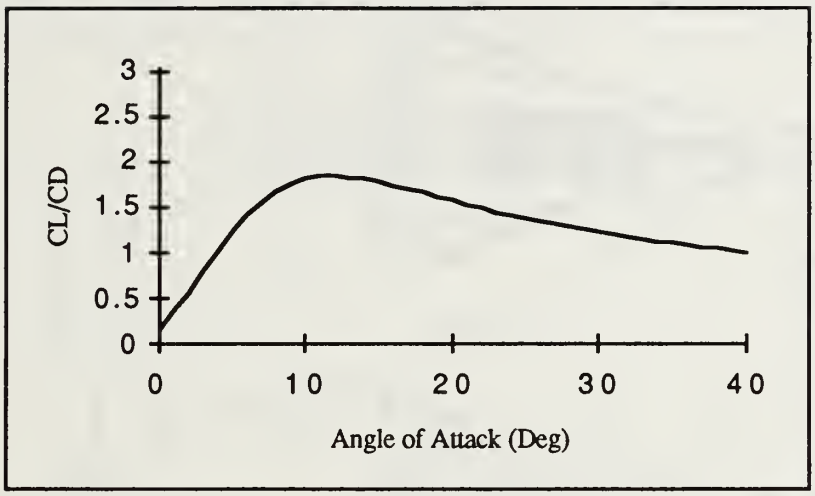

Figure 7. C_L/C_D vs Angle of Attack for ERV

B. MANEUVERABLE REENTRY RESEARCH VEHICLE

Although the MRRV is similar in size and weight to the ERV, that is where the similarity ends. The MRRV has a maximum lift to drag ratio on the order of 2.6, much higher than the ERV. Figure 8 show a three-view sketch of the MRRV and when compared to Figure 4 the differences between the MRRV and the ERV become apparent. The MRRV is a much more slender design; the slenderness ratio of the fuselage is approximately one eighth. The overall length is 7.62 m and because of the sharper design of the vehicle it has an effective wing area of 11.7 square meters, 4.7 square meters less than the ERV. The propulsion system is identical to the ERV using three Marquardt R-40-B rocket motors, providing a total of 14679 Newtons of thrust at a specific impulse of 295 seconds. [Ref. 3: p. 7]

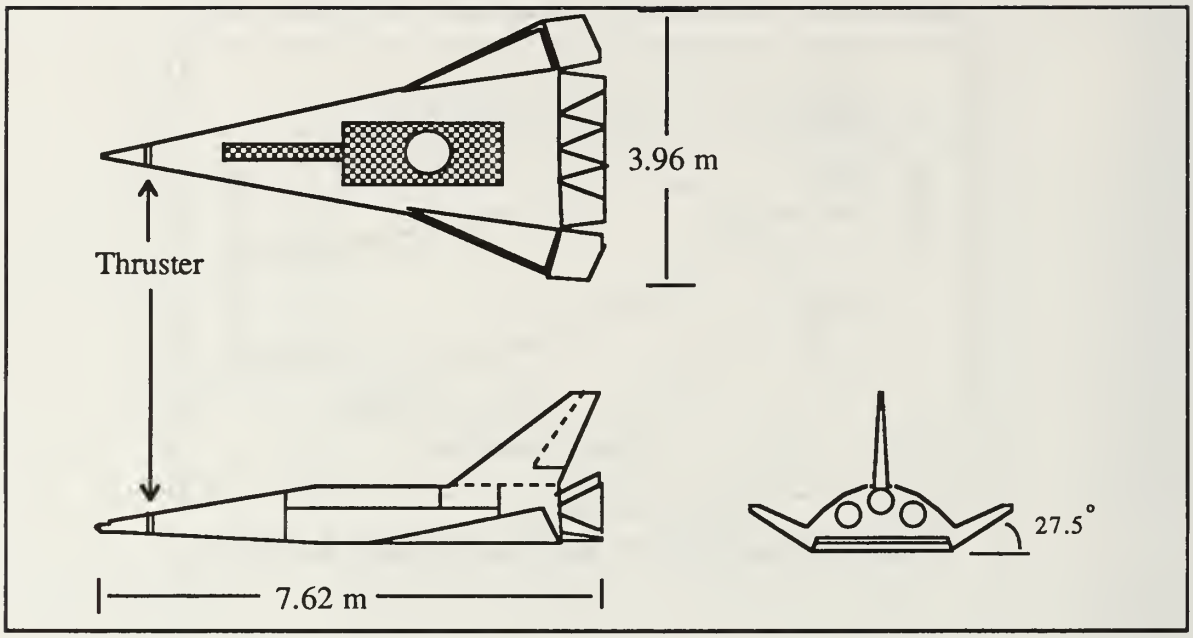

Figure 8. Three-view Diagram of MRRV

The method used to find the coefficient of lift and drag curves for the ERV was employed to find those for the MRRV. Figure 9 shows a plot of the curve fit for the coefficient of lift with the wind tunnel data obtained for the MRRV, and Figure 10 displays the coefficient of drag. It is interesting to note that even though Figure 11 shows the MRRV to have a higher lift to drag ratio than the ERV, a comparison of the actual coefficient of lift and drag show the ERV to have higher actual values. The lower lift and drag coefficients coupled with the decreased wing area of the MRRV will be of importance during the analysis to follow.

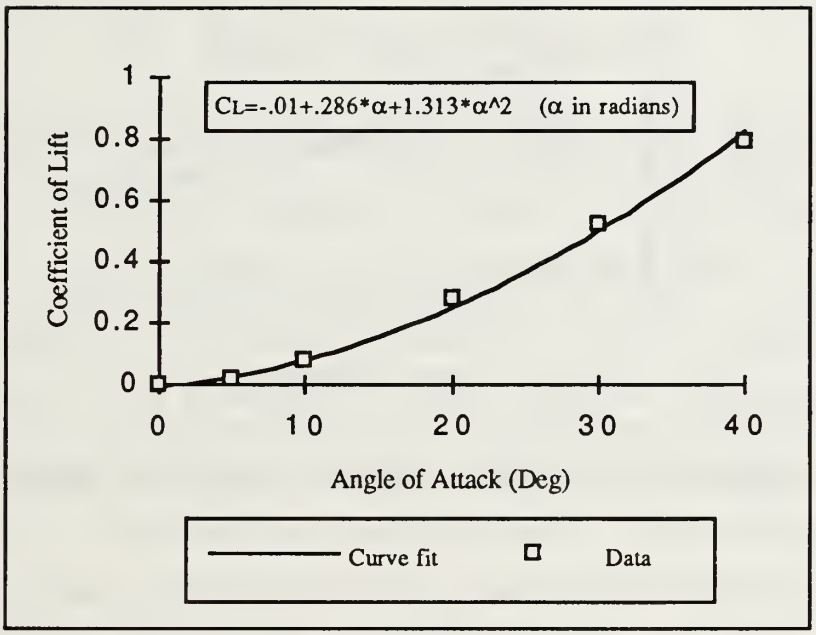

Figure 9. Coefficient of Lift vs Angle of Attack for MRRV

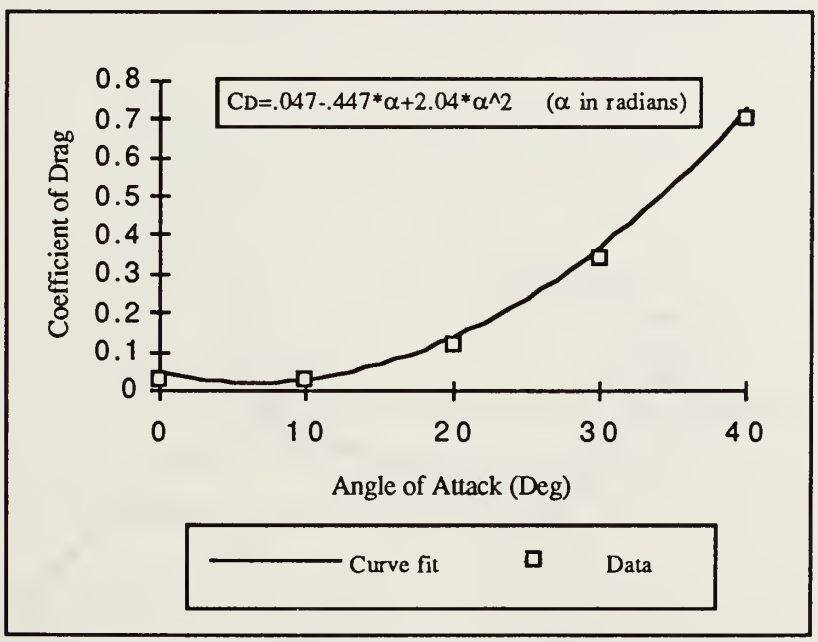

Figure 10. Coefficient of Drag vs Angle of Attack for MRRV

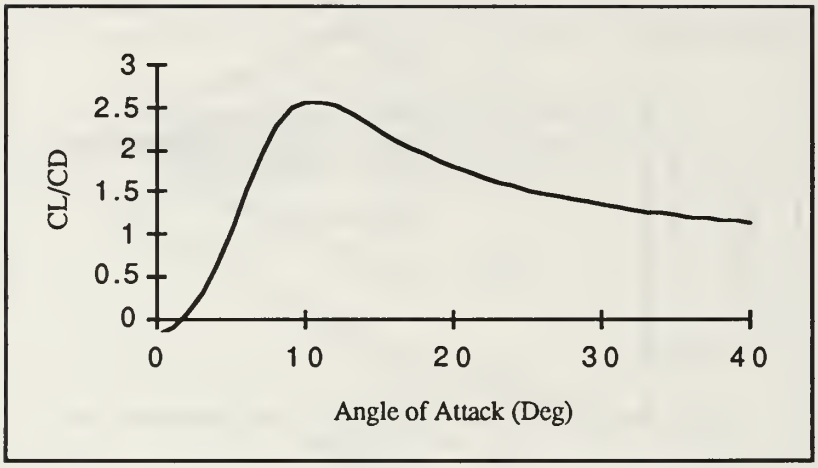

Figure 11. C_L/C_D vs Angle of Attack for MRRV

III. EQUATIONS OF MOTION

The equations of motion for a hypervelocity lifting body are derived, free of singularities. Six specific variables are utilized to describe the spacecraft's position and velocity. Referenced to an inertial frame XYZ, the vehicle's position is represented by spherical coordinates r (radius), θ (right ascension), and ϕ (declination) and the vehicle's motion as speed V, and direction by the angles γ (flight path angle) and ψ (heading angle). The flight path angle, γ, is positive above the local horizon and negative below. The heading angle is the angle the horizontal projection of the velocity vector makes with the local

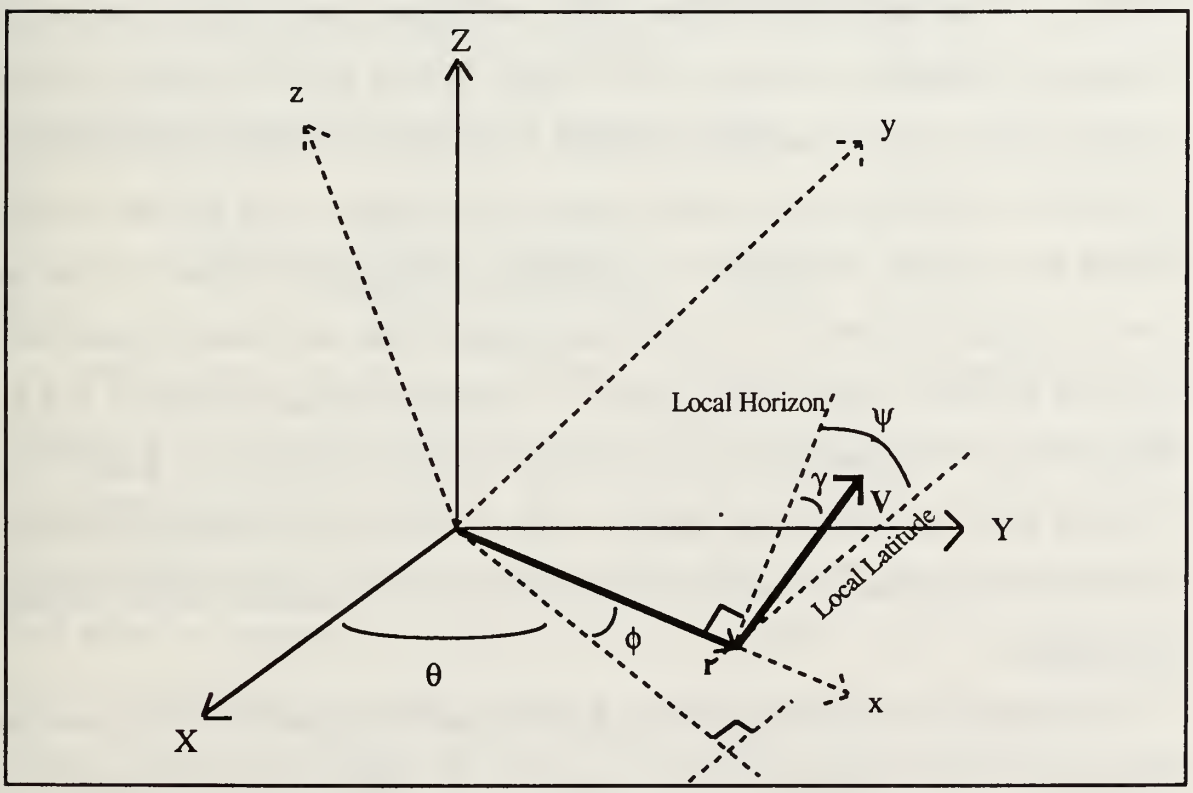

Figure 12. Graphical Representation of Variables

latitude. Figure 12 graphically shows the six variables and their relationship to each other.

Assumptions made in the derivation of these equations are: a spherical, non-rotating, Earth and negligible atmospheric winds. The Earth's oblateness is not considered due to the short nature of the atmospheric interaction by the spacecraft. Future studies may find a need to include these effects. Additionally, the thrust vector of the spacecraft was assumed to be in line with its longitudinal axis.

A. DERIVATION OF EQUATIONS

Three coordinate systems are defined for the derivation of the equations of motion. The inertially fixed system, XYZ. A rotating system, xyz, in which the origin is coincident with that of the inertial system and the positive x axis remains fixed to the spacecraft. Finally, a system x'y'z' which is fixed to the spacecraft with the y' axis oriented along the velocity vector and the x' axis within the xy plane, the origin of the system lies at the end of the radius vector in the xyz system, (Figure 12). The transformation from the inertial system into the xyz system is done using a body 3-2 rotation through angles θ and ϕ respectively. Additionally, to obtain the xyz system from the x'y'z' a body 3-1 rotation must be done using angles γ and ψ. Using the following DCMs (direction cosine matrix) all of the parameters can be described in the rotating xyz system.

The DCM for the transformation from the inertial system to xyz system is expressed as the multiplication of two matrices the right matrix representing the body-3 rotation and the left matrix representing the body-2 rotation

$$\begin{bmatrix} x \\ y \\ z \end{bmatrix} = \begin{bmatrix} \cos\phi & 0 & \sin\phi \\ 0 & 1 & 0 \\ -\sin\phi & 0 & \cos\phi \end{bmatrix} \begin{bmatrix} \cos\theta & \sin\theta & 0 \\ -\sin\theta & \cos\theta & 0 \\ 0 & 0 & 1 \end{bmatrix} \begin{bmatrix} X \\ Y \\ Z \end{bmatrix} \tag{3.1}$$

Consolidating the two matrix transformations for a body 3-2 rotation, we have

$$\begin{bmatrix} x \\ y \\ z \end{bmatrix} = \begin{bmatrix} \cos\theta\cos\phi & \sin\theta\cos\phi & \sin\phi \\ -\sin\theta & \cos\theta & 0 \\ -\cos\theta\sin\phi & -\sin\theta\sin\phi & \cos\phi \end{bmatrix} \begin{bmatrix} X \\ Y \\ Z \end{bmatrix} \tag{3.2}$$

Similarly, the DCM for the transformation from the x'y'z' spacecraft system to xyz system is expressed below:

$$\begin{bmatrix} x \\ y \\ z \end{bmatrix} = \begin{bmatrix} 1 & 0 & 0 \\ 0 & \cos\psi & -\sin\psi \\ 0 & \sin\psi & \cos\psi \end{bmatrix} \begin{bmatrix} \cos\gamma & \sin\gamma & 0 \\ -\sin\gamma\cos\gamma & 0 & \\ 0 & 0 & 1 \end{bmatrix} \begin{bmatrix} x' \\ y' \\ z' \end{bmatrix} \tag{3.3}$$

Completing the algebra the body 3-1 rotation, we get,

$$\begin{bmatrix} x \\ y \\ z \end{bmatrix} = \begin{bmatrix} \cos\gamma & \sin\gamma & 0 \\ -\sin\gamma\cos\psi & \cos\gamma\cos\psi & -\sin\psi \\ -\sin\gamma\sin\psi & \cos\gamma\sin\psi & \cos\psi \end{bmatrix} \begin{bmatrix} x' \\ y' \\ z' \end{bmatrix} \tag{3.4}$$

For a system of equations to completely describe the spacecraft's motion and position at any moment in time, an equation of the time derivative for each of the six variables must be established. By equating the spacecraft's velocity vector to the time derivative of the spacecraft's position vector, the derivatives for r, θ, and ϕ can be expressed as functions of r, θ, ϕ, V, γ, and ψ. The time derivatives for V, γ, and ψ are also found by taking the time derivative of the spacecraft's velocity vector and equating them to the forces acting on the spacecraft using the relationship $\vec{F} = m_a \vec{a}$.

The vectors for the spacecraft's position and velocity in the xyz system are

$$\vec{r} = r\,\hat{i} \tag{3.5}$$

and

$$\widehat{Vj'} = V \sin\gamma\,\hat{i} + V\cos\gamma\cos\psi\,\hat{j} + V\cos\gamma\sin\psi\,\hat{k} \tag{3.6}$$

Additionally, the angular velocity of the spacecraft is

$$\vec{\Omega} = \sin\phi\,\frac{d\theta}{dt}\,\hat{i} - \frac{d\phi}{dt}\,\hat{j} + \cos\phi\,\frac{d\theta}{dt}\,\hat{k} \tag{3.7}$$

Taking the derivative of Equation 3.5, yields an equivalent velocity vector,

$$\vec{V} = \frac{d\vec{r}}{dt}_{XYZ} = \frac{d\vec{r}}{dt}\,\hat{i} + (\vec{\Omega}\times\vec{r}) = \frac{d\vec{r}}{dt}\,\hat{i} + r\cos\phi\,\frac{d\theta}{dt}\,\hat{j} + r\,\frac{d\phi}{dt}\,\hat{k} \tag{3.8}$$

Equating the components of Equations 3.6 and 3.8 gives the first three equations of motion. These three equations describe the spacecraft's position in spherical coordinates for any time

$$\frac{dr}{dt} = V\sin\gamma \tag{3.9}$$

$$\frac{d\theta}{dt} = \frac{V\cos\gamma\cos\psi}{r\cos\phi} \tag{3.10}$$

$$\frac{d\phi}{dt} = \frac{V\cos\gamma\sin\psi}{r} \tag{3.11}$$

Similarly taking the derivative of the velocity vector (Equation 3.6) the final three equations of motion can be found. The last three equations will describe the spacecraft's movement through space at any particular time.

$$\frac{d\vec{V}}{dt} = \frac{d(V\sin\gamma)}{dt}\,\hat{i} + V\sin\gamma\,\frac{d\hat{i}}{dt} + \frac{d(V\cos\gamma\cos\psi)}{dt}\,\hat{j}$$

$$+ V\cos\gamma\cos\psi\,\frac{d\hat{j}}{dt} + \frac{d(V\cos\gamma\sin\psi)}{dt}\,\hat{k} + V\cos\gamma\sin\psi\,\frac{d\hat{k}}{dt}$$

Expanding, we have

$$\frac{d\vec{V}}{dt} = \left[\sin\gamma\frac{dV}{dt} + V\cos\gamma\frac{d\gamma}{dt}\right]\hat{i} + \left[V\sin\gamma\left(\cos\phi\frac{d\theta}{dt}\hat{j} + \frac{d\phi}{dt}\hat{k}\right)\right]$$
$$+ \left[\cos\gamma\cos\psi\frac{dV}{dt} - V\cos\psi\sin\gamma\frac{d\gamma}{dt} - V\cos\gamma\sin\psi\frac{d\psi}{dt}\right]\hat{j}$$
$$+ \left[V\cos\gamma\cos\psi\left(-\cos\phi\frac{d\theta}{dt}\hat{i} + \sin\phi\frac{d\theta}{dt}\hat{k}\right)\right]$$
$$+ \left[\cos\gamma\sin\psi\frac{dV}{dt} - V\sin\psi\sin\gamma\frac{d\gamma}{dt} + V\cos\gamma\cos\psi\frac{d\psi}{dt}\right]\hat{k}$$
$$+ \left[V\cos\gamma\sin\psi\left(-\frac{d\phi}{dt}\hat{i} - \sin\phi\frac{d\theta}{dt}\hat{j}\right)\right] \qquad (3.12)$$

Replacing $d\theta/dt$ and $d\phi/dt$ in Equation 3.12 using Equations 3.10 and 3.11 yields

$$\frac{d\vec{V}}{dt} = \left[\sin\gamma\frac{dV}{dt} + V\cos\gamma\frac{d\gamma}{dt} - \frac{V^2\cos^2\gamma\cos^2\psi}{r} - \frac{V^2\cos^2\gamma\sin^2\psi}{r}\right]\hat{i}$$
$$+ \left[\cos\gamma\cos\psi\frac{dV}{dt} - V\cos\psi\sin\gamma\frac{d\gamma}{dt} - V\cos\gamma\sin\psi\frac{d\psi}{dt}\right.$$
$$\left. + \frac{V^2\sin\gamma\cos\gamma\cos\psi}{r} - \frac{V\cos^2\gamma\sin\psi\cos\psi\tan\phi}{r}\right]\hat{j}$$
$$+ \left[\cos\gamma\sin\psi\frac{dV}{dt} - V\sin\psi\sin\gamma\frac{d\gamma}{dt} + V\cos\gamma\cos\psi\frac{d\psi}{dt}\right.$$
$$\left. + \frac{V^2\sin\gamma\cos\gamma\sin\psi}{r} + \frac{V^2\cos^2\gamma\cos^2\psi\tan\phi}{r}\right]\hat{k} \qquad (3.13)$$

The forces acting on the spacecraft in the x'y'z' coordinate system can be expressed as (Figure 13)

$$F_{x'} = (T\sin\alpha + L)\cos\sigma \qquad (3.14)$$

$$F_{y'} = T\cos\alpha - D \qquad (3.15)$$

$$F_{z'} = (T\sin\alpha + L)\sin\sigma \qquad (3.16)$$

Restating the fundamental equation of motion as a derivative of velocity with respect to time

$$\vec{F} = m_a \vec{a} = m_a \frac{d\vec{V}}{dt} \tag{3.17}$$

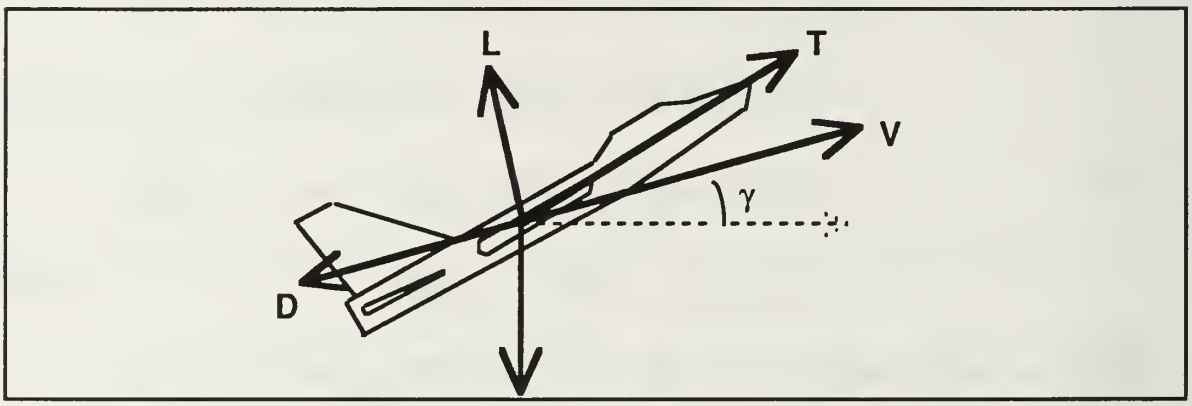

Figure 13. Spacecraft Forces During Atmospheric Interaction

Using the DCM from Equation 3.3 the forces from the spacecraft's frame of reference (x'y'z') can be transformed into the rotating frame of reference (xyz) using

$$\begin{bmatrix} F_x \\ F_y \\ F_z \end{bmatrix} = \begin{bmatrix} \cos\gamma & \sin\gamma & 0 \\ -\sin\gamma\cos\psi & \cos\gamma\cos\psi & -\sin\gamma \\ -\sin\gamma\sin\psi & \cos\gamma\sin\psi & \cos\psi \end{bmatrix} \begin{bmatrix} F_{x'} \\ F_{y'} \\ F_{z'} \end{bmatrix} \tag{3.18}$$

With the above transformation matrix and using Equations 3.14, 3.15, and 3.16, the forces acting on the spacecraft can be expressed in the rotating system as

$$F_x = (T\sin\alpha + L)\cos\sigma\cos\gamma + (T\cos\alpha - D)\sin\gamma - m_a g \tag{3.19}$$

$$F_y = -(T\sin\alpha + L)\cos\sigma\sin\gamma\cos\psi + (T\cos\alpha - D)\cos\gamma\cos\psi - (T\sin\alpha + L)\sin\sigma\sin\psi \tag{3.20}$$

and

$$F_z = -(T\sin\alpha + L)\cos\sigma\sin\gamma\sin\psi$$

$$+ (T\cos\alpha - D)\cos\gamma\sin\psi - (T\sin\alpha + L)\sin\sigma\cos\psi \qquad (3.21)$$

Now setting the components of Equation 3.17 equal to the spacecraft force equations expressed in the rotating coordinate system, three independent equations are obtained for evaluation and reduction namely

$$\hat{i}: (T\sin\alpha + L)\cos\sigma\cos\gamma + (T\cos\alpha - D)\sin\gamma - m_a g =$$

$$m_a\left[\sin\gamma\frac{dV}{dt} + V\cos\gamma\frac{d\gamma}{dt} - \frac{V^2\cos^2\gamma}{r}\right] \qquad (3.22)$$

$$\hat{j}: -(T\sin\alpha + L)\cos\sigma\sin\gamma\cos\psi + (T\cos\alpha - D)\cos\gamma\cos\psi$$

$$-(T\sin\alpha + L)\sin\sigma\sin\psi = m_a\left[\cos\gamma\cos\psi\frac{dV}{dt} - V\cos\psi\sin\gamma\frac{d\gamma}{dt}\right.$$

$$\left. - V\cos\gamma\sin\psi\frac{d\psi}{dt} + \frac{V^2}{r}\cos\gamma\cos\psi(\sin\gamma - \cos\gamma\sin\psi\tan\phi)\right] \qquad (3.23)$$

$$\hat{k}: -(T\sin\alpha + L)\cos\sigma\sin\gamma\sin\psi + (T\cos\alpha - D)\cos\gamma\sin\psi$$

$$+(T\sin\alpha + L)\sin\sigma\cos\psi = m_a\left[\cos\gamma\sin\psi\frac{dV}{dt} - V\sin\psi\sin\gamma\frac{d\gamma}{dt}\right.$$

$$\left. + V\cos\gamma\cos\psi\frac{d\psi}{dt} + \frac{V^2}{r}\cos\gamma(\sin\gamma\sin\psi + \cos\gamma\cos^2\psi\tan\phi)\right] \qquad (3.24)$$

In order to obtain the last three equations of motion, Equations 3.22, 3.23, and 3.24 must be algebraically manipulated and reduced. Taking Equation 3.23 and multiplying by cos(ψ) and Equation 3.24 and multiplying by sin(ψ), then adding the two resulting equations together gives

$$(T\cos\alpha - D) - m_a g\sin\gamma = m_a\frac{dV}{dt} \qquad (3.25)$$

Substituting this result back into Equation 3.22 and reducing yields

$$V\frac{d\gamma}{dt} = \frac{(T \sin\alpha + L)\cos\sigma - m\,g\cos\gamma}{m_a} + \frac{V^2}{r}\cos\gamma \tag{3.26}$$

A final substitution into Equation 3.23 gives us the sixth equation of motion for the flight vehicle, namely

$$V\frac{d\psi}{dt} = \frac{(T \sin\alpha + L)\sin\sigma}{m_a \cos\gamma} - \frac{V^2}{r}\cos\gamma\cos\psi\tan\phi \tag{3.27}$$

Making one final reduction by defining variables A_R, A_S, and A_W which are the components of the acceleration of the flight vehicle in the radial, tangential, and binormal directions respectively, we have from Equations 3.14, 3.15, and 3.16,

$$A_R = \frac{(T \sin\alpha + L)\cos\sigma}{m_a} \tag{3.28}$$

$$A_S = \frac{T\cos\alpha - D}{m_a} \tag{3.29}$$

and

$$A_W = \frac{(T \sin\alpha + L)\sin\sigma}{m_a} \tag{3.30}$$

The last three equations of motion can now be written as

$$\frac{dV}{dt} = A_S - g\sin\gamma \tag{3.31}$$

$$V\frac{d\gamma}{dt} = A_R + \left(\frac{V^2}{r} - g\right)\cos\gamma \tag{3.32}$$

and

$$V\frac{d\psi}{dt} = \frac{A_W}{\cos\gamma} + \frac{V^2}{r}\cos\gamma\cos\psi\tan\phi \tag{3.33}$$

B. DERIVATION OF THE INCLINATION

The six equations of motion, Equations 3.9-3.11 and 3.31-3.33, when integrated numerically yield the spacecraft's position in spherical coordinates at any time during the orbit. For facilitating a comparison between orbits, a relationship between the orbital elements and the spherical coordinates is necessary. In non-coplanar transfers, an orbital element which indicates performance of the maneuver is inclination. The necessity to convert from spherical coordinates to inclination of the orbit for the purpose of performance evaluation is the basis for this derivation. As shown in Equations 3.5 and 3.6 the radius and velocity vectors can be written in terms of the rotating frame of reference. The angular momentum vector ($\vec{h}$) is defined as the cross product of the radius and the velocity vector; thus

$$\vec{h} = \vec{r} \times \vec{V} = - V r \cos\gamma \sin\psi \hat{j} + V r \cos\gamma \cos\psi \hat{k} \tag{3.34}$$

The magnitude of the momentum vector is, consequently

$$|\vec{h}| = \sqrt{(V r)^2 \cos^2\gamma \sin^2\psi + (V r)^2 \cos^2\gamma \cos^2\psi} \tag{3.35}$$

giving

$$|\vec{h}| = V r \cos\gamma \tag{3.36}$$

The inclination of an orbit is defined as the the angle between the angular momentum vector and $\vec{k}$, the direction of the Z axis of the inertial coordinate system. The inclination can be found by defining $\vec{k}$ within the rotating xyz system and then using the dot product definition to find the angle between the $\vec{h}$ and the $\vec{k}$ vectors. Since

$$\vec{k} = \sin\phi \hat{i} + \cos\phi \hat{k} \tag{3.37}$$

$$\vec{h} \cdot \vec{k} = |\vec{h}| \cos i \tag{3.38}$$

and

$$V\, r \cos\gamma \cos\psi \cos\phi = |\vec{h}| \cos i \tag{3.39}$$

Utilizing Equations 3.36 and 3.39, the cosine of the inclination can be found explicitly in terms of ψ and ϕ, thus

$$\cos i = \cos\psi \cos\phi \tag{3.40}$$

This result, exhibits no constraint on whether the path of the orbiting vehicle is Keplerian or not.

IV. CONTROL LAWS

Aerocruise and aerobang each have unique methods for controlling the space vehicle's trajectory during an atmospheric encounter. Aerocruise uses two distinct rules to maintain the proper flight path. First, the spacecraft's velocity is controlled by setting the component of thrust in the direction of travel to exactly counteract the vehicle's drag. Second, the altitude is maintained constant by modulating the flight vehicle's angle of bank. This is done by balancing the vertical component of the lift and thrust to the vehicle's weight minus the centrifugal force. The method of control used by the aerobang maneuver is less complicated, in that only one parameter of the flight vehicle is modulated during the maneuver. The angle of bank during the aerobang maneuver is set at a constant value, typically 90 degrees; this maximizes the inclination change caused by the aerodynamic lift. Additionally, the thrust is not modulated but set to the maximum available thrust. The modulated parameter is the flight vehicle's angle of attack, and the spacecraft is not constrained by a particular speed or altitude, but to the maximum allowable heating rate.

A. AEROCRUISE CONTROL LAW

Early investigations of the aerocruise maneuver dictated that superior results could be achieved if the spacecraft operated at $(L/D)_{max}$ [Ref. 3: p. 5]. The development of the control law for the angle of bank required to maintain a constant altitude and velocity, and hence a constant heating rate, utilizes this concept. Counterbalancing the drag on the flight vehicle with the thrust produced demands a prediction of the drag encountered at various altitudes. The

density in the U.S. Standard Atmosphere, 1976, [Ref. 11: p. 7] is approximated by an exponential behavior in the altitude range from 50 km to 120 km, namely

$$\rho = \rho_s e^{-\beta(r-r_s)} \tag{4.1}$$

where

$$\rho_s = 3.0968\times10^{-4} \text{ kg/m}^3$$

$$\beta = 1.41\times10^{-4} \text{ m}^{-1}$$

$$r_s = 6438 \text{ km}$$

This density approximation coupled with the speed of the spacecraft and the coefficient of drag on the vehicle, at $(L/D)_{max}$, yields a drag force which is constant throughout the aerocruise maneuver. Looking back at Figure 13, the thrust required for aerocruise to balance the drag force by the component of thrust along the spacecraft's direction of motion is given by

$$T = \frac{D}{\cos\alpha} \tag{4.2}$$

where

$$D = \frac{1}{2}\rho V^2 S C_D \tag{4.3}$$

In order to calculate the required angle of bank for the aerocruise maneuver it is necessary to look at Equations 3.28 and 3.32, which are repeated here for convenience

$$A_R = \frac{(T\sin\alpha + L)\cos\sigma}{m_a} \tag{3.28}$$

$$V\frac{d\gamma}{dt} = A_R + \left(\frac{V^2}{r} - g\right)\cos\gamma \tag{3.32}$$

The flight path of the vehicle during the aerocruise maneuver is circular and thus the flight path angle (γ) is zero and will remain zero throughout the maneuver.

Combining this information, with the substitution of Equation 3.28 into Equation 3.32 and solving for the angle of bank (σ) yields

$$\sigma = \cos^{-1}\left[\frac{m_a \left(g - \frac{V^2}{r} \right)}{(T \sin \alpha + L)} \right] \tag{4.4}$$

Obviously, from Equation 4.4, the angle of bank becomes 90 degrees when the spacecraft's velocity is equal to the velocity required to maintain a circular orbit at the given altitude. As the speed of the spacecraft becomes higher than circular speed, the angle of bank also increases beyond 90 degrees, causing the lift vector to be directed Earthward to maintain the circular path of the vehicle. Likewise, as the spacecraft's velocity decreases below circular speed, the angle of bank decreases and the lift vector is directed upward to sustain the circular path. Examining Equation 4.4, it is clear that there is a limitation in the angle of bank which can be used to control the flight path; this limitation occurs when the absolute value of the terms within the square bracket exceeds 1. In this case, there is not enough lift generated to maintain the desired flight path. To correct for this condition, the vehicle would have to abandon flight at $(L/D)_{max}$ and choose a higher angle of attack in order to generate the necessary lift.

B. AEROBANG CONTROL LAW

Differing from the aerocruise method, the aerobang maneuver allows the vehicle to vary the altitude and velocity in order to maintain a constant heating rate on the spacecraft. In order to determine how the angle of attack is modulated to keep the flight vehicle at a constant heating rate, the modeling of the heating rate must first be discussed. Heating rate is modeled as a function of atmospheric density (ρ) and vehicle speed (V), by the expression [Ref. 9: p. 291],

$$\dot{Q} = k \rho^n V^m \tag{4.5}$$

where K, n, and m are constants.

Coupling Equation 4.5 with Equation 4.1, the exponential atmospheric model, the speed of the spacecraft can be shown to be a function of the vehicle's geocentric radius for any given heating rate. Equation 4.6 shows this relationship and is the basis for the aerobang control law.

$$V = \left[\frac{\dot{Q}_o}{k \rho_o^n e^{-\beta n (r - r_o)}} \right]^{\frac{1}{m}} \tag{4.6}$$

The derivative with respect to time of Equation 4.6 is necessary in order to couple the equations of motion for the spacecraft to the constant heating rate flight path. Thus,

$$\frac{dV}{dt} = \left[\frac{\dot{Q}_o}{k \rho_o^n} \right]^{\frac{1}{m}} e^{-\frac{\beta n}{m} r_o} \left[\frac{\beta n}{m} \right] e^{-\frac{\beta n}{m} r} \frac{dr}{dt} \tag{4.7}$$

$$\frac{dV}{dt} = \left[\frac{\beta n}{m} \right] V \frac{dr}{dt} \tag{4.8}$$

Combining Equation 3.9 with Equation 4.8, dr/dt can be eliminated and dV/dt can be expressed as a function of V and γ

$$\frac{dV}{dt} = \left[\frac{\beta n}{m} \right] V^2 \sin \gamma \tag{4.9}$$

Substituting Equation 3.29 into Equation 3.31 and eliminating the variable A_S, another equation for dV/dt is derived (Equation 4.10). The two Equations, 4.9 and 4.10, yield a final relationship

$$\frac{dV}{dt} = \frac{T \cos \alpha - D}{m_a} - g \sin \gamma \tag{4.10}$$

Equations 4.9 and 4.10 together enable the evaluation of the angle of attack for any given flight condition, from the equation

$$0 = T \cos \alpha - D - m_a \sin \gamma \left(g + \frac{\beta n}{m} V^2 \right) \equiv f(\alpha) \tag{4.11}$$

However, since the drag term, D, is also a function of α, solving for α is not as straightforward as it might at first appear.

1. Mechanics of Convergence

Equation 4.11 is made up of three distinct terms, a thrust component, a drag component, and a component which depends on the vehicle's velocity and flight path angle. The first two of these terms are dependent on the angle of attack of the vehicle, while the third term remains constant for a given flight condition, independent of the angle of attack. Figure 14 graphically show the relationship of these terms in solving for the angle of attack of the flight vehicle. The terms which contain the flight path angle and the drag are summed and

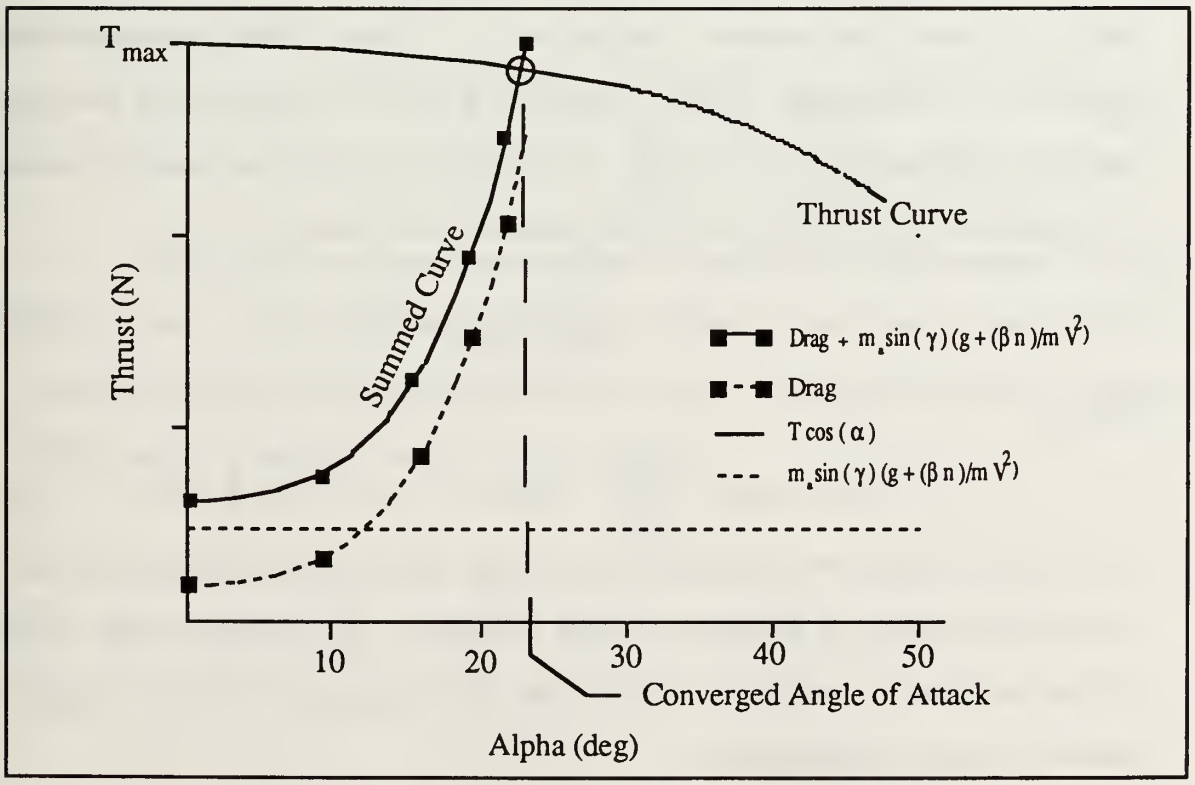

Figure 14. Graphical Example of Angle of Attack Solution

plotted together with the thrust term, the intersection of these two lines occur at the proper angle of attack to maintain a flight path along a constant heating rate line.

For a given flight vehicle, the thrust curve shown in Figure 14 is fixed for any flight condition, while the drag and flight path terms increase with increasing flight speed. As the flight speed continues to increase, the converged angle of attack needed to maintain a stable flight path decreases, and at some point there exists a flight condition where the two curves would not intersect. At this point, the thrust curve lies below the curve representing the sum of the drag and flight path terms, and no solution exists for an angle of attack.

2. Newton's Method of Convergence

The nature of Equation 4.11 does not allow a direct solution for the angle of attack, and another method must be used. An iterative process developed by Sir Isaac Newton lends itself well to applications involving computer methods [Ref. 12: p. 142]. The method involves following the tangent of the function down to the zero of the function as expressed by

$$\alpha_{n+1} = \alpha_n - \frac{f(\alpha_n)}{f'(\alpha_{n+1})}, \quad f'(\alpha_n) \neq 0 \tag{4.12}$$

where,

$$f'(\alpha) = -T \sin\alpha - \frac{dD}{d\alpha} = -T \sin\alpha - (C_5 + 2 C_6 |\alpha|) \frac{1}{2} \rho V^2 S \tag{4.13}$$

and C_5 and C_6 are the coefficients of the first order and second order terms in the binomial curve fit of drag vs. angle of attack. The iterative nature of this process requires an accurate initial guess for the angle of attack in order to reduce the time of computation.

3. Initial Guess of Angle of Attack

Properly setting the initial angle of attack close to the correct value can significantly decrease the required number of iterations needed to converge to the solution. The method employed here involves simplifying the information already presented in order to obtain a direct solution. Two assumptions are made in order to provide this starting point for the solution of α. These two assumptions are that initially the acceleration component in the tangential direction is nearly zero and that the angle of attack is small enough that its cosine is approximately unity. Applying these two simplifications in Equation 3.29 leaves the expression that thrust (T) equals the drag (D). Therefore

$$\frac{T}{\frac{1}{2}\rho V^2 S} = C_4 + C_5 \alpha + C_6 \alpha^2 \tag{4.14}$$

yielding the solution

$$\alpha = \frac{C_5 + \sqrt{C_5^2 + 4\left[\frac{T}{\frac{1}{2}\rho V^2 S} - C_4\right] C_6}}{2 C_6} \tag{4.15}$$

While this is only an approximation, it enables the initial angle of attack to start closer to the solution than if some arbitrary value for α were selected. As will be shown later, these assumptions are close to the actual value for a flight vehicle with a circular or near circular velocity.

V. PROGRAM DEVELOPMENT

A computer program was developed using VAX FORTRAN to simulate a lifting body within the atmosphere. The program utilized a fourth order Runge-Kutta routine to integrate the differential equations of motion derived in Chapter III. Equations of motion for the simulation were left in a dimensional form because the accuracy of the computations was considered adequate using double precision variables within the program. The limited gain in accuracy and computational time using non-dimensional equations and programing techniques was considered insufficient to justify the increased time for implementing the equations in a non-dimensional form. Redundant checks were made both internal and external to the program to ensure the integration time step of the Runge-Kutta routine was kept small enough to insure the accuracy of the program.

The program was written in a modular format with the main program controlling six subroutines. Three of the subroutines, CNTRL, ACEL, and ORB, deal with the flight mechanics of the spacecraft. Two of the subroutines, HDR and WRT, control the output of the program and the last subroutine, RK4, is a standard fourth order Runge-Kutta routine. The source code of the program is given in Appendix A.

A. MAIN PROGRAM

The main program, pages 68 through 70 of Appendix A, acts as a control center for the subroutines, and computations within the main program are kept to a minimum. Only the calculation of the spacecraft mass is done within

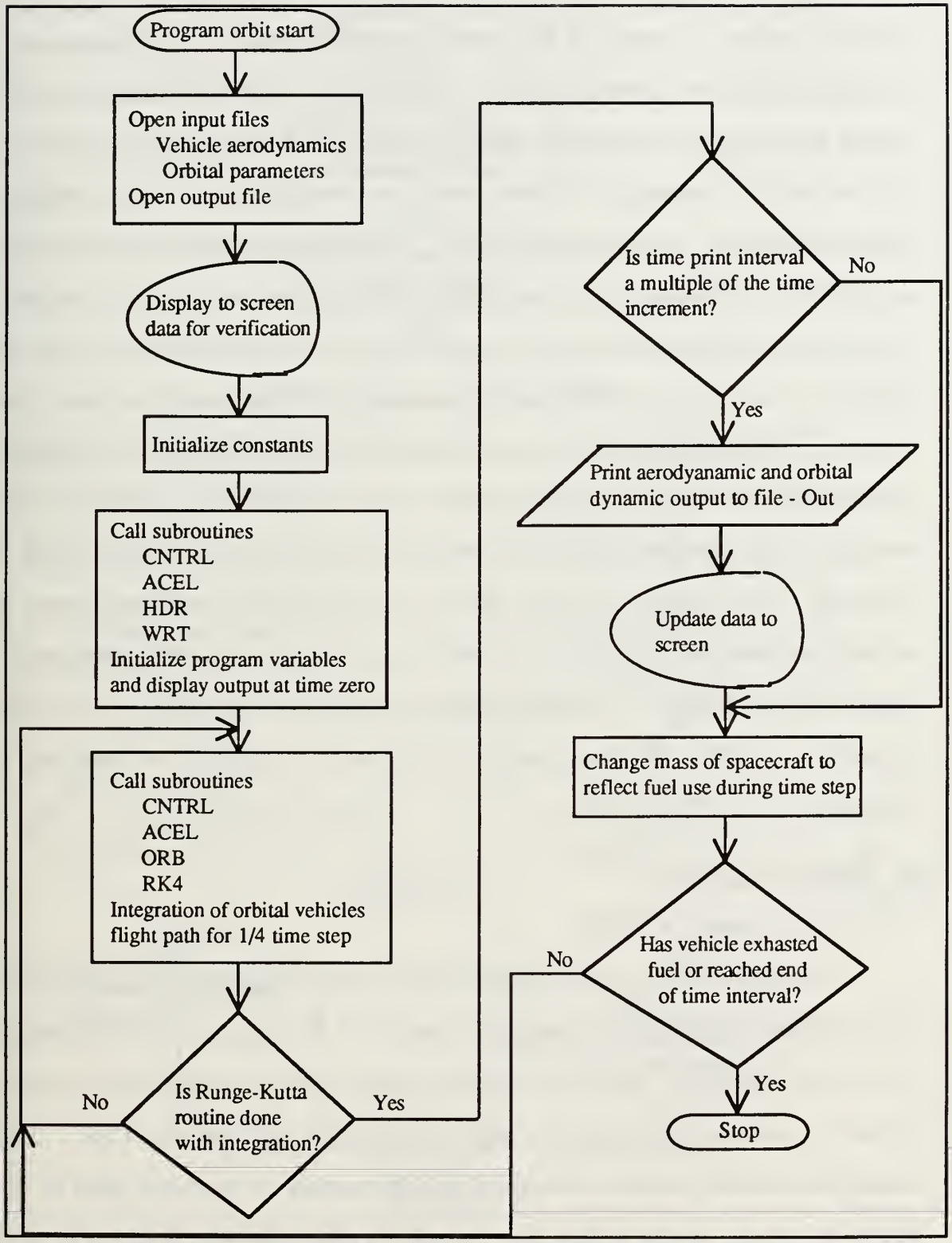

Figure 15. Flow Chart for Main Program

the main program. Figure 15 is a flow chart of the main program operations. Two input files were used in order to separate the orbital parameters from the vehicle aerodynamic parameters. Sample input files are included in Appendix A. One output file was used for both a hard copy text and input into a separate graphics program. A quick health check of the program was displayed to the terminal for verification of proper inputs and progress through the program. The first call to subroutine CNTRL and ACEL are for output purposes only, the values at time zero are displayed in the output file after calling these two routines. The main loop of the program proceeds through the aerodynamic, atmospheric, and orbital dynamic models at each integration time step, the time interval is then compared with the time print interval and an output written if necessary. The last part of the loop is to change the spacecraft mass in accordance with the time interval, thrust on the spacecraft, and the specific impulse of the rockets. A double check is used to determine the end of the program: if either the final time or final mass is reached, the program is terminated.

B. SUBROUTINES

1. Subroutine CNTRL

This subroutine, as the acronym implies, deals with the control laws used for the different atmospheric interaction models. A flow chart of this subroutine is shown in Figure 16. Both the aerobang and aerocruise models were included in the subroutine and each was accessed through the variable CSE. The atmospheric model, which is common to both models, is executed prior to the control functions. A test is then done in order to determine which model to turn

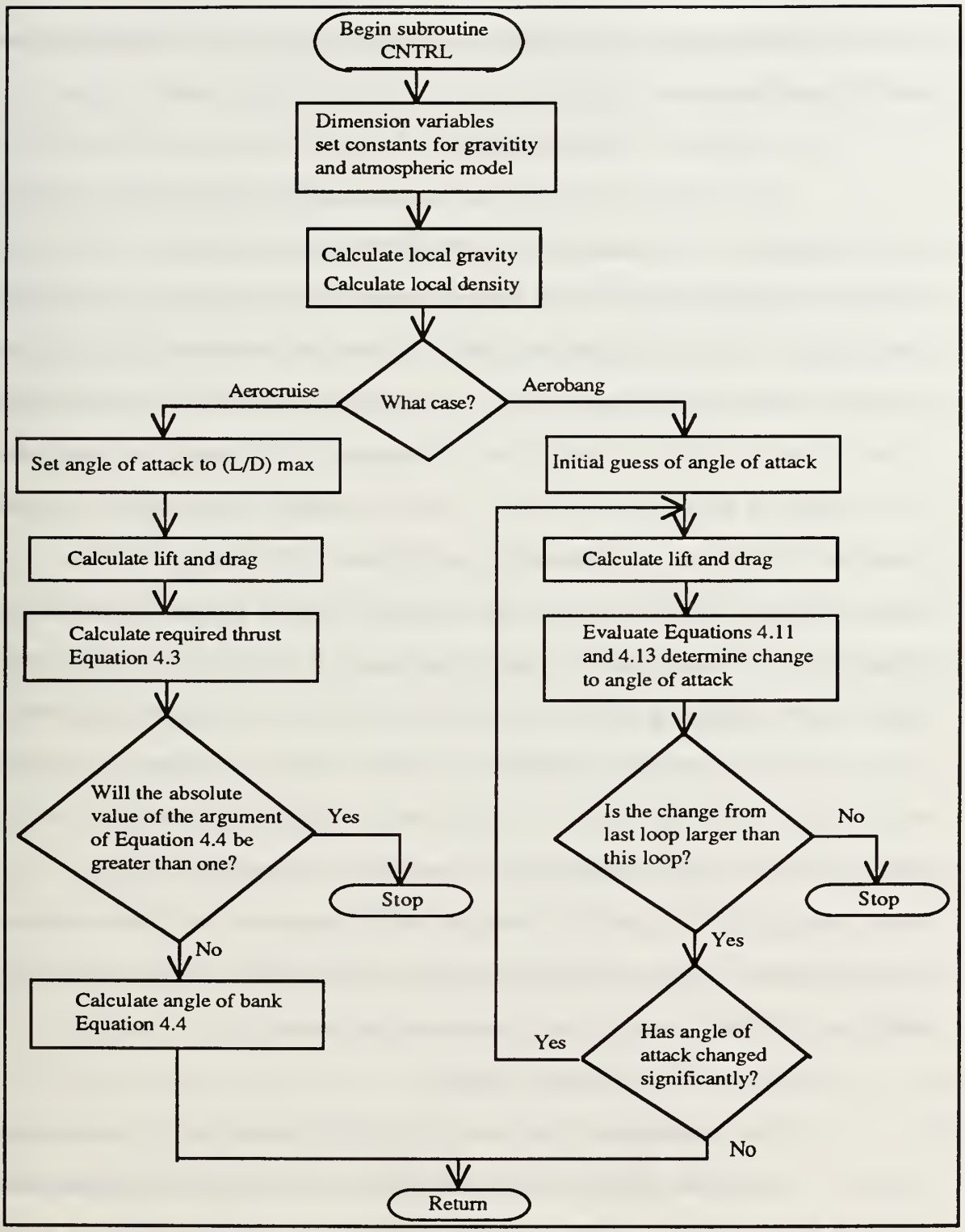

Figure 16. Flow Chart of CNTRL Subroutine

on; for convenience, the order of discussion will be the same as their appearance within the subroutine.

a. Aerobang Control Model

This model is made up three distinct parts. The first part calculates an initial guess of the angle of attack for the flight vehicle. While the convergence routine will converge on the correct angle of attack using any initial guess, a good first guess is determined to decrease the computation time of the program. The second portion of the convergence routine uses Newton's method of convergence. First, the coefficients of drag and lift for the flight vehicle for a given angle of attack are computed. This information is then used to calculate the value of the $f(\alpha)$ in, Equation 4.11, and its derivative using, Equation 4.13. These two values dictate the change in the angle of attack and the whole process is repeated until there is little change to the angle of attack in sequential loops. The final part of the model is an automatic internal check. It is quite possible for the model to have no angle of attack on which to converge. Two possibilities exist for this happening: one, the model is unable to maintain a constant heating rate for the given flight conditions and two, that the integration step size is too large, forcing the vehicle off the constant heating rate curve. If there were no check within the routine, the output would be questionable, or, the routine might enter into an infinite loop looking for a nonexistent answer.

b. Aerocruise Control Model

The second model within the CNTRL subroutine incorporates Equations 4.3 and 4.4. The model sets the angle of attack for $(L/D)_{max}$ and lift and drag are calculated. Using this drag prediction, the thrust is set to a value which will exactly match the drag. Using all these values, the angle of bank

necessary for circular flight is found. A check is also done to assure that there is an angle of bank which will satisfy the given flight conditions; if one does not exist, then the program is stopped at this point .

2. Subroutine ACEL

This simple routine computes the accelerations on the flight vehicle, excluding gravity, using Equations 3.28-30. These equations have been isolated within their own subroutine for future program users. Accelerations experienced by the flight vehicle during a maneuver can be evaluated using the information provided by this routine.

3. Subroutine ORB

Subroutine ORB calculates the differential values contained within the equations of motion derived in Chapter III. These equations are defined within the subroutine using the dimensioned variables X and XDOT. This is done in order to make it easier to pass the variables and their derivatives to the Runge-Kutta routine and to make the routine more generic in nature.

4. Subroutines HDR and WRT

These are the output subroutines and HDR is called only once during each execution of the program. The subroutine HDR prints the header at the top of the output file. This header contains some of the selected input data in order that one may readily associate the conditions that created it. The subroutine WRT prints the output data and is called at every time print interval as specified by the user. It is necessary to limit printing of the output to every 1000 to 2000 integration time steps in order not to be overloaded with minutiae.

5. Subroutine RK4

This subroutine was taken from the public domain collection of fortran subroutines held at the Naval Postgraduate School. It was written by Professor I. M. Ross and is a standard fourth order Runge-Kutta routine. It is used by passing the computed values for the variables and their derivatives to the routine via the variables X and XDOT. The routine actually requires four passes for the integration of one time step and during each of these four passes, the program goes back and recalculates the variables X and XDOT. The variable INDEX keeps track of the looping requirements for this routine.

C. PROGRAM USAGE

Proper operation of the program requires the manipulation of two input files. As previously mentioned, one file, AERO.DAT, contains the aerodynamic inputs and DATA.DAT contains the orbital dynamic inputs. The output file, OUT.DAT, contains the time history of ten important variables used in the analysis of the orbital plane changes. To set up a run, the user must first edit the AERO.DAT file to reflect the aerodynamics of the flight vehicle. The file AERO.DAT contains fifteen variables; each variable and the corresponding unit is explained in Table 1. The second file DATA.DAT corresponds to the starting conditions of the flight vehicle. The file DATA.DAT contains eleven input variables all of which are contained in Table 2 along with the meanings of the variable and the necessary units. Once these two files have been set for the particular flight vehicle, the program ORBIT can be executed to obtain a time history output of the maneuver.

TABLE 1. INPUT FILE AERO.DAT

Variable	Meaning and Required Units
Coefficient C1	Zero order coefficient for binomial curve fit of C_L vs alpha.
Coefficient C2	First order coefficient for binomial curve fit of C_L vs alpha.
Coefficient C3	Second order coefficient for binomial curve fit of C_L vs alpha.
Coefficient C4	Zero order coefficient for binomial curve fit of C_D vs alpha.
Coefficient C5	First order coefficient for binomial curve fit of C_D vs alpha.
Coefficient C6	Second order coefficient for binomial curve fit of C_D vs alpha.
AOA for $(C_L/C_D)_{max}$ (AOPT)	Angle of Attack for $(C_L/C_D)_{max}$, Radians
AOB for Bang Maneuver (AOB)	Angle of Bang used during the Aerobang Maneuver, Radians.
Density Exponent (N)	Exponent of density within the heating rate model, Equation 4.5.
Velocity Exponent (M)	Exponent of velocity within the heating rate model, Equation 4.5.
Reference Area (S)	Flight vehicle reference area, used in lift and drag calculations, square meter
Initial Mass (MASS0)	Flight vehicle mass at beginning of maneuver, kg.
Final Mass (FM)	Final mass of vehicle at end of maneuver, kg.
Specific Impulse (SPI)	Specific Impulse of propulsion system, seconds.
Thrust (N)	Total thrust developed by propulsion system, or thrust used during Aerobang maneuver, Newtons.

TABLE 2. INPUT FILE DATA.DAT

Variable	Meaning and Required Units
Case (CSE)	Designate the type of model to be used.
Radius (R)	Geocentric radius of spacecraft body, units are in meters.
Declination (θ)	Spherical coordinate angular measurement in radians, see Figure 12.
Right Ascension (ϕ)	Spherical coordinate angular measurement in radians, see Figure 12.
Speed (V)	Speed of spacecraft, units are in meters per second.
Flight Path Angle (γ)	Measure of spacecraft attitude referenced to local horizon, units in radians.
Heading Angle (ψ)	Measure of spacecraft attitude referenced to the earth's equator, units in radians.
Begin Time (T)	Start of simulation, units in seconds.
End Time (TF)	End of simulation, units in seconds.
Time Interval	Integration time step, units in seconds.
Print Time Interval (TPI)	Interval at which call is made to output subroutine, units in seconds.

D. PROGRAM VALIDATION

The program was validated in two ways, the first method involved testing the orbital mechanics portion of the program and the second method involved matching data output from a previously run problem. For the orbital mechanics validation all of the aerodynamic and thrust parameters were set to zero, while the control models were turned off and the flight velocity and altitude were set to a known orbital condition. The values output from the computer program were then compared to the calculated values. The comparison is summarized in Table 3. As the data show, there is no appreciable difference between the calculated values and the computer output values.

TABLE 3. ORBITAL DYNAMIC VALIDATION

	Calculated Value	Program Value
Apogee	6675.0 km	6675.0 km
Apogee Velocity	7.700 km/sec	7.700 km/sec
Period	5370 sec	5375 sec
Eccentricity	.007123	.007129
Perigee	6580.5 kn	6580.5 km
Perigee Velocity	7.810 km	7.810 km

The second phase of the validation involved matching the solution from the present computer program to a previously published solution using the same inputs. For this phase an aerocruise maneuver was simulated using the full capabilities of the program.

TABLE 4. PROGRAM VALIDATION

	Value From Cervisi [Ref. 13]	Program Value
Velocity	7.254 km/sec	7.254 km/sec
Radius of Orbit	6447.5 km	6447.5 km
Initial/Final Mass	4762.7/2948.4 kg	4762.7/2948.2 kg
Initial/Final AOB	52.4/67.8 degrees	52.37/67.8 degrees
Inclination Change	16.83 degrees	16.87 degrees

Reference 13 contains enough data to reconstruct the the necessary inputs for an accurate simulation. The data taken from the article was all in a non-dimensional format and it was necessary to take it back to a dimensional form for use in the program, ORBIT. Both outputs are summarized in Table 4 and as can been seen, they match very closely.

VI. ANALYSIS

Evaluation of the data gathered from modeling the atmospheric interaction of the two chosen flight vehicles will determine for what flight conditions the aerobang method is superior to the aerocruise. The analysis will demonstrate the similarity of the two control methods and the fact that the aerocruise model may be thought of as an aerobang maneuver constrained to a particular altitude and angle of attack.

A. FORMULATION OF THE SOLUTION

The objective was to conduct a numerical investigation into the efficiency of both the aerocruise and aerobang control laws. Efficiency of the maneuver is defined as the inclination change a maneuver produces for a given amount of fuel expended. The effects of three separate parameters on the efficiency of each maneuver were studied. The three parameters were the flight vehicle speed, the $(L/D)_{max}$ of the vehicle, and the stagnation heating rate. In short, the maneuvers were conducted over a varying range of flight velocities for two different heating rates using first the ERV and then the MRRV.

Flight vehicle velocities ranged from super- to subcircular velocities. The terms super- and subcircular are defined as faster or slower than the circular orbital velocity at that particular altitude. A parameter k can be defined as

$$k = \frac{V_c}{V} \tag{6.1}$$

which is the ratio of the circular speed (V_c) to the flight speed. Thus, $k>1$ is subcircular speed and $k<1$ is supercircular speed. These two ranges are of interest because the control law for the aerobang maneuver dictates that at

supercircular speeds, the flight vehicle gains altitude, while at subcircular speeds, it might lose altitude. If the maneuver proves to be more efficient at supercircular speeds, the increase in altitude and velocity would only add to the efficiency by requiring less fuel to reorbit the spacecraft at termination of the atmospheric interaction. On the other hand, if the aerobang maneuver proves to be more efficient at subcircular speeds, a further analysis must be conducted to account for the loss in altitude and velocity. In this study, the altitude was maintained using two different methods. The first method involved giving the flight vehicle a small positive flight path angle, rather than a zero flight path angle; the upward tendency of the trajectory would offset the altitude loss by the maneuver. The second method was to tilt the angle of bank using some of the lift for the inclination change to keep the flight vehicle at a constant altitude.

The maneuver simulations were conducted for two different heating-rate values in order to determine the effect different altitudes and velocities would have on the model of each maneuver. The heating rates were chosen to be $0.9088*10^6$ and $1.42*10^6$ Watts per square meter, referenced to a 1-ft radius sphere [Ref. 7: p. 490]. For the ERV, the maximum heating rate value would correspond a stagnation temperature of 4180 degrees Fahrenheit during a plane change maneuver lasting 1500 seconds [Ref. 14: pp. 278-9]. To effect an equitable comparison of the two flight vehicles using the same flight profiles, these heating rate values were also imposed on the MRRV, though the MRRV is designed to handle higher heating rates [Ref. 6: p. 516].

It is noted that the values of k selected for evaluation varied for each flight vehicle and for different heating rates. In order to evaluate the aerocruise and

aerobang maneuvers during similar flight condition the k values for the simulations are confined to a subset of flight speeds common to both maneuvers.

B. SUPERCIRCULAR PROFILES

1. High Heating Rate

a. ERV

A stagnation heating rate of $1.42*10^6$ watts per square meter was taken for the ERV. Simulations were run for two different supercircular speeds corresponding to values of k from .94 and .95. Each run was allowed to expend fuel up to 2% of the initial mass. The aerobang maneuver in either case did not

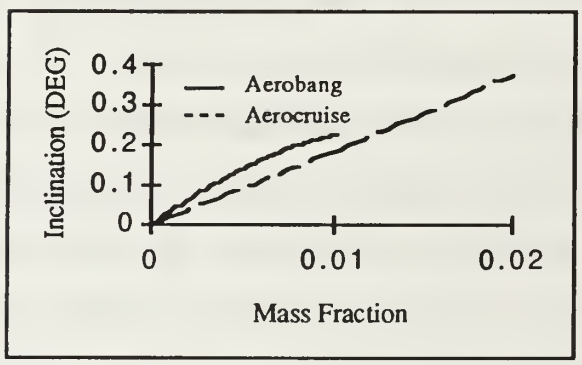

Figure 17. Inclination Change for ERV k=.94

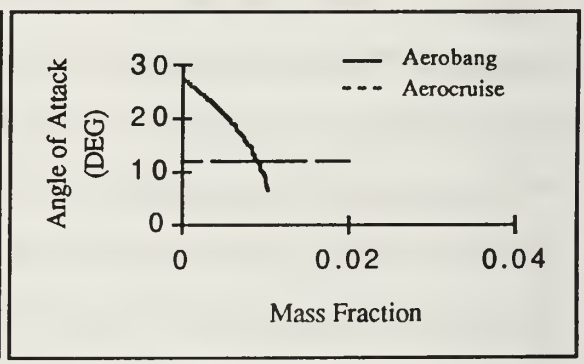

Figure 18. Angle of Attack vs Mass Fraction ERV k=.94

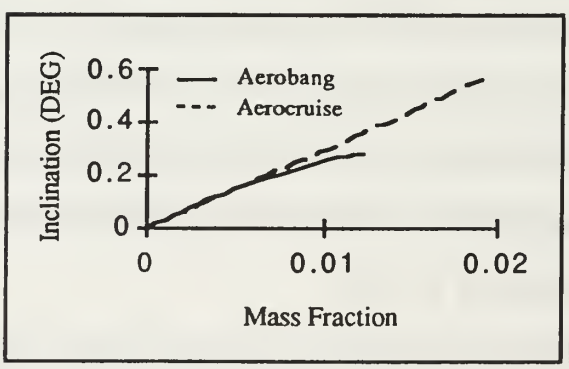

Figure 19. Inclination Change for ERV k=.95

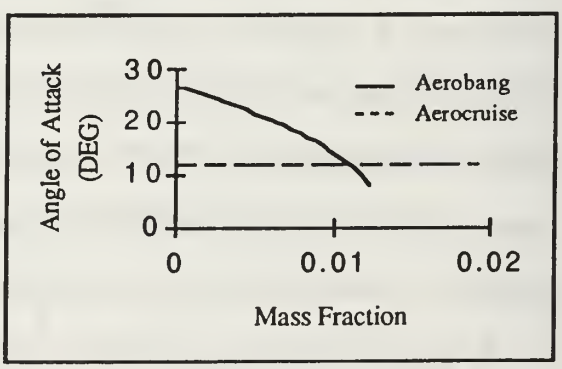

Figure 20. Angle of Attack vs Mass Fraction for ERV k=.95

complete the full 2% mass expenditure. The maneuver was unable maintain the constant heating rate curve, thus terminating the flight profile. As shown in Figures 17 and 19 the aerobang maneuver did display a more efficient process of inclination change as compared to the aerocruise maneuver for supercircular speeds.

For k=.94, the aerobang maneuver terminated at 1% mass fraction with a .226 degree inclination change, while the aerocruise achieved only .186 degrees inclination change. At .75% mass fraction the inclination difference was at a maximum of .05 degrees. A strategy for maximizing inclination change would be to conduct multiple passes thought the atmosphere such that at each pass, the flight profile would be terminated at the point of maximum inclination change difference. The k=.95 flight profile displays similar characteristics to the k=.94 case except that the aerobang maneuver became less efficient at approximately .5% mass fraction of fuel. At lower values of fuel mass fraction the inclination change for the aerobang and aerocruise maneuvers were nearly indistinguishable from each other.

No cases for k<.94 were run because of the inability of the aerocruise control law to maintain a constant heating rate while flying at the angle of attack corresponding to $(L/D)_{max}$. The aerocruise control law required angles of bank of 134 and 153 degrees for the k=.95 and the k=.94 cases respectively. For k=.93, the force required to balance the centrifugal force of the flight vehicle exceeded the lift generated, making it impossible for the flight vehicle to maintain the desired heating rate. In contrast, the aerobang maneuver could be executed under the restrictions/specifications of higher orbital speeds. A limitation encountered in the aerobang maneuver is that at faster speeds, the

angle of attack decreases to zero sooner, making the length of the maneuver shorter.

Another difference in these two maneuvers is found in the time to complete the maneuver for a specified mass fraction of fuel. The aerobang maneuver is completed four times faster than the aerocruise maneuver for the same mass fraction burned. This observation has two implications: first, the aerobang maneuver can be completed closer to the node of the orbit giving the maneuver an additional increase in efficiency for long flight profiles, and second, the integrated heat load on the spacecraft is lower for the aerobang maneuver. The temperature of the vehicle will depend on the total heat brought into the vehicle minus the heat which can be dissipated away; if the heat load can be reduced, this would decrease the average temperature of the spacecraft. The reduced time of flight to complete an increased inclination change therefore implies that the aerobang maneuver could possibly allow flight profiles to be executed at a higher heating rate than the aerocruise maneuver, since the integrated heat load would be less, granting that the materials can handle the higher heating rate.

b. MRRV

The MRRV velocities were simulated from values of k from .99 to .98. No speeds greater than k=.98 were simulated due to the fact that the aerocruise maneuver could not generate the required lift at $(L/D)_{max}$. All the simulations required fuel up to 2% of the spacecraft mass. Observing Figures 21 through 23, it is clear that the aerobang maneuver is more efficient at producing an inclination change somewhere between k=.99 and k=.985. The thrust required to execute the maneuver using the aerobang method was 20 times

greater than the aerocruise method. This thrust differential is passed on to the time of flight required for each maneuver as the aerobang method required only 19.3 seconds to expend the 2% fuel while it took over 400 seconds for each of the aerocruise cases. The thrust of the aerocruise maneuver is based on the drag encountered, while the MRRV has a high $(L/D)_{max}$ the actual drag force is low requiring only a small amount of thrust.

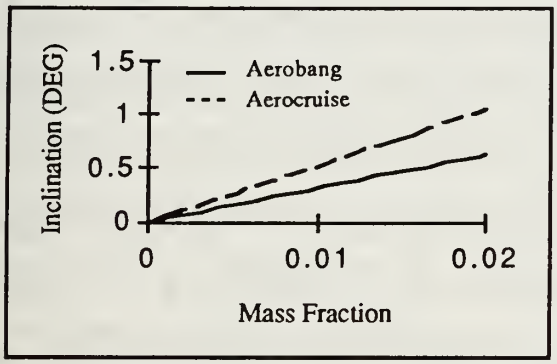

Figure 21. Inclination Change for MRRV k=.99

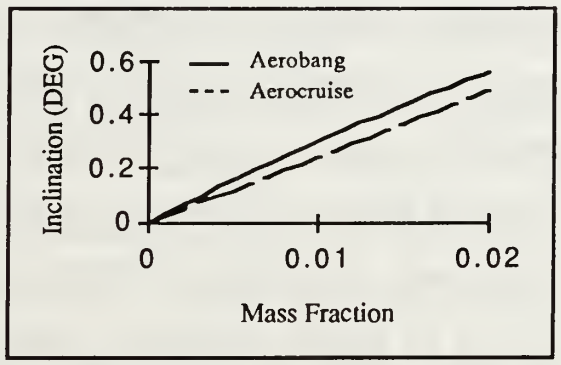

Figure 22. Inclination Change for MRRV k=.985

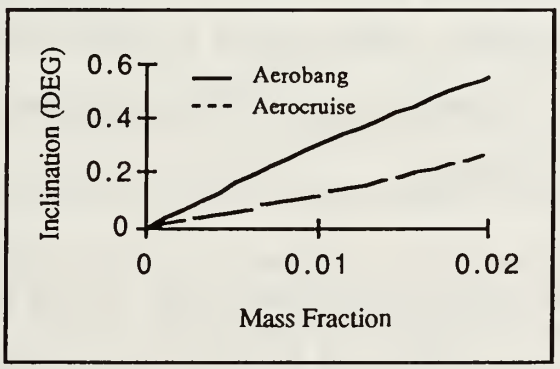

Figure 23. Inclination Change for MRRV k=.98

2. Low Heating Rate

a. ERV

Simulations were conducted up to a mass fraction of 2% for fuel expended and a stagnation heating rate of $0.9088*10^6$ watts per square meter

referenced to a 1 foot diameter sphere. This lower heating rate corresponds to a higher altitude and lower speed for the flight vehicle. The aerocruise simulation was unable to maintain altitude for k<.97 due to inadequate lift generated at $(L/D)_{max}$. The aerobang maneuver was able to expend all of the 2% mass fraction under these conditions. At k=.97, the aerobang maneuver once again proved to be more efficient at generating inclination change, with a total inclination change of .454 degrees at the end of the simulation. The point of maximum inclination difference between the aerocruise method and the aerobang method occurred at approximately 1% mass fraction, with the aerobang maneuver having a .265 degrees inclination change and the aerocruise maneuver having only .212 degrees inclination change. As an example, for k=.97 and a desired 10 degree inclination change, an aerobang maneuver would save approximately 490 kg of fuel using a multiple pass technique. Additionally, the time involved to conduct the aerocruise maneuver is almost nine times greater than the aerobang method. While there is a region of supercircular velocities where the aerocruise maneuver is more efficient than aerobang, it occurs nearer the circular velocity or k=1.

b. MRRV

The low heating rate flight profile for the MRRV was flown for speeds corresponding to k=.990 and k=.997. These velocities are very close to the circular orbital velocity. At the increased altitude and reduced velocity, as compared to the high heating rate simulation of section B.1.ii, the lift generated by the lifting body is reduced even further. Each of the aerocruise maneuvers require over 900 seconds to complete for a maximum inclination change of 1.1 degrees at k=.997. The aerocruise maneuver exceeds the aerobang maneuver in

inclination change efficiency until sometime before the velocity exceeds the k=.995 level. Once again, the range in which the efficiency of the aerocruise method is superior is limited to a band close to the circular orbital velocity and beyond this band the aerobang method becomes increasingly more efficient.

C. SUBCIRCULAR PROFILES

Unlike the supercircular velocities the subcircular region requires more analysis to truly determine which method of inclination change is more efficient. Execution of the aerobang maneuver using a subcircular profile always appears to be more efficient but causes the spacecraft to lose altitude. This altitude loss must be made up for in order to effect an equitable comparison between the two maneuvers. Both methods of altitude maintenance discussed in the above section are utilized here to bring the vehicle back to nearly the same initial velocity and altitude.

1. High Heating Rate

a. ERV

The ERV simulation was conducted for values of k=1.03 to k=1.1. Table 5 summarizes the data from these flight profiles. Column one of the table is the standard aerobang maneuver; column two is the aerobang maneuver using a positive flight path angle to return the flight vehicle to the original altitude at the end of the 2% mass fraction fuel expenditure; column three is the aerobang maneuver using an angle of bank to maintain a particular altitude, and column four is the aerocruise maneuver for which the comparison is made. Observing Table 5, the aerobang maneuver displays expected results: the efficiency of the maneuver remains higher than that of the aerocruise maneuver, but with an

TABLE 5. SUMMARY OF ERV FLIGHT PROFILES FOR HIGH HEATING RATE

	K= 1.03 HEATING RATE		1.42*10^6 WATTS/M^2	
	AEROBANG	AEROBANG	AEROBANG	AEROCRUISE
Initial Gamma	0 deg	0.046 deg	0 deg	0 deg
Initial AOB	90 deg	90 deg	83.4 deg	73.3 deg
Inclination change	0.93 deg	0.754 deg	0.765 deg	0.849 deg
Mass Fraction used	2%	2%	2%	2%
Change in Altitude	-124 m	4 m	-2 m	0 m
Time required	20.5 sec	20.5 sec	20.5 sec	57.9 sec
fuel/degree inclination	111.83 kg/deg	137.93 kg/deg	135.95 kg/deg	122.5 kg/deg
% difference over Aerocruise	8.71 %	-12.60 %	-10.98 %	0 %
	K= 1.05 HEATING RATE		**1.42*10^6 WATTS/M^2**	
	AEROBANG	AEROBANG	AEROBANG	AEROCRUISE
Initial Gamma	0 deg	0.072 deg	0 deg	0 deg
Initial AOB	90 deg	90 deg	80 deg	65 deg
Inclination change	1.05 deg	0.779 deg	0.794 deg	0.821 deg
Mass Fraction used	2%	2%	2%	2%
Change in Altitude	-196 m	0 m	-9 m	0 m
Time required	20.5 sec	20.5 sec	20.5 sec	53.3 sec
fuel/degree inclination	99.05 kg/deg	133.5 kg/deg	130.98 kg/deg	126.67 kg/deg
% difference over Aerocruise	21.80 %	-5.39 %	-3.40 %	0 %
	K= 1.07 HEATING RATE		**1.42*10^6 WATTS/M^2**	
	AEROBANG	AEROBANG	AEROBANG	AEROCRUISE
Initial Gamma	0 deg	0.097 deg	0 deg	0 deg
Initial AOB	90 deg	90 deg	77 deg	58.3 deg
Inclination change	1.166 deg	0.794 deg	0.823 deg	0.787 deg
Mass Fraction used	2%	2%	2%	2%
Change in Altitude	-264 m	-2 m	-15 m	0 m
Time required	20.5 sec	20.5 sec	20.5 sec	49.1 sec
fuel/degree inclination	89.19 kg/deg	130.98 kg/deg	126.37 kg/deg	132.15 kg/deg
% difference over Aerocruise	32.51 %	0.89 %	4.37 %	0 %
	K= 1.1 HEATING RATE		**1.42*10^6 WATTS/M^2**	
	AEROBANG	AEROBANG*	AEROBANG	AEROCRUISE
Initial Gamma	0 deg	0.101 deg	0 deg	0 deg
Initial AOB	90 deg	90 deg	71 deg	50.6 deg
Inclination change	1.336 deg	0.969 deg	0.816 deg	0.736 deg
Mass Fraction used	2%	2%	2%	2%
Change in Altitude	-360 m	-97 m	1 m	0 m
Time required	20.5 sec	20.5 sec	20.5 sec	43.6 sec
fuel/degree inclination	77.84 kg/deg	107.33 kg/deg	127.45 kg/deg	141.3 kg/deg
% difference over Aerocruise	44.91 %	24.04 %	9.80 %	0 %

attached altitude penalty. The altitude penalty increases as the percentage difference over the aerocruise maneuver increases. At k=1.03 the altitude loss is 124 m while the difference over aerocruise is 8.7%; this increases at k=1.1 to an altitude loss of 360 m with a difference of 44.9%. As shown in Figure 24 the

most effective method of altitude maintenance utilizes the angle of bank. The angle of bank method can be used over a much larger range of flight speeds than the flight path angle method; the flight path method cannot to be used beyond k=1.07 because no angle of attack solution exists for this combination of variables. From Figure 24, the aerobang maneuver that uses the angle of bank for altitude maintenance becomes more efficient than the aerocruise method at speeds less than k=1.06. As an example, for k=1.1 a 20 degree inclination change using the aerobang method augmented with angle of bank would use 277 kg of fuel less than aerocruise maneuver.

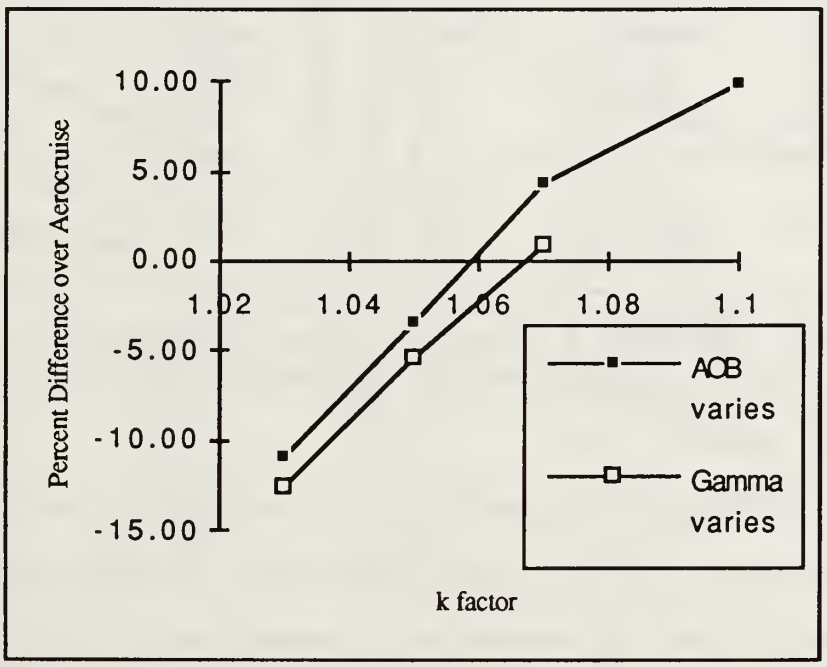

Figure 24. Fuel Percent Difference over Aerocruise vs k Factor for ERV (High Heating Rate)

Unlike the supercircular case in which the angle of attack during the aerobang maneuver steadily decreases to zero, in the subcircular case, it increases as the flight vehicle descends. The angle of attack could possibly exceed the stall angle of the flight vehicle, terminating the maneuver

prematurely. An unexpected advantage experienced during the angle-of-bank augmented aerobang maneuver is that the angle of attack remains constant throughout the maneuver, similar to the aerocruise maneuver, except the angle of attack is fixed at a higher value. This was observed in all cases where the aerobang maneuver was augmented with the angle of bank. Figures 25 and 26 graphically show this concept. Figure 25 shows the inclination versus mass fraction for the aerobang maneuver at k=1.1 and Figure 26 shows the inclination change for the same maneuver augmented with an angle of bank of 71 degrees.

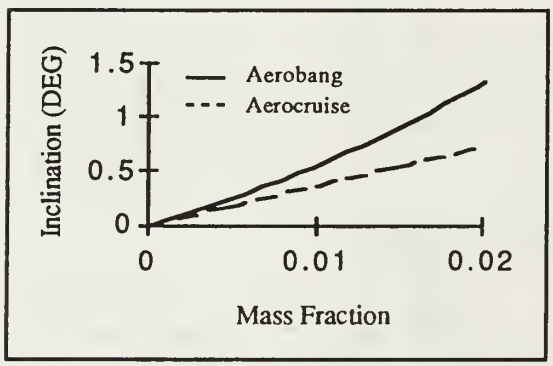

Figure 25. ERV k=1.1 Angle of Attack Profile unaugmented

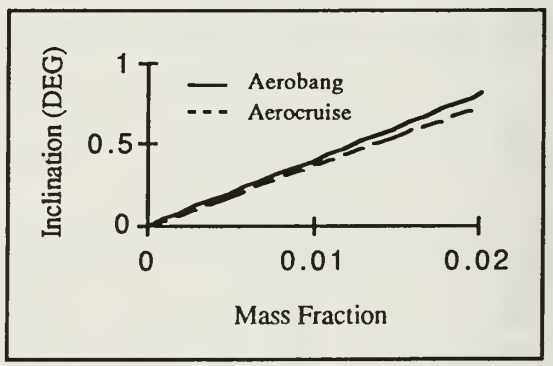

Figure 26. ERV k=1.1 Angle of Attack Profile AOB augmented

b. MRRV

The range of speeds at which the MRRV could be flown was significantly reduced when compared to the ERV. The parameter, k, ranged in value from 1.01 to 1.02; beyond 1.02 the speed was too slow to provide the necessary lift to maintain the aerocruise maneuver. This same effect was seen for the supercircular flight profiles. Table 6 summarizes the data obtained from the simulations conducted. Under these conditions, the efficiency of the flight path angle method of altitude maintenance was essentially identical to the angle of bank method. This may be attributed to the narrow range of flight velocities

sampled, all of which are closer to circular orbital velocity than the those sampled in the ERV case.

TABLE 6. SUMMARY OF MRRV FLIGHT PROFILES FOR HIGH HEATING RATE

	K= 1.01 HEATING RATE		1.42*10^6 WATTS/M^2	
	AEROBANG	AEROBANG	AEROBANG	AEROCRUISE
Initial Gamma	0 deg	0.017 deg	0 deg	0 deg
Initial AOB	90 deg	90 deg	87.2 deg	58.5 deg
Inclination change	0.74 deg	0.682 deg	0.682 deg	0.994 deg
Mass Fraction used	2%	2%	2%	2%
Change in Altitude	-44 m	1 m	0 m	0 m
Time required	19.3 sec	19.3 sec	19.3 sec	353.4 sec
fuel/degree inclination	132.43 kg/deg	143.70 kg/deg	143.70 kg/deg	98.59 kg/deg
% difference over Aerocruise	-34.32 %	-45.75 %	-45.75 %	0.00 %
	K= 1.015 HEATING RATE		**1.42*10^6 WATTS/M^2**	
	AEROBANG	AEROBANG	AEROBANG	AEROCRUISE
Initial Gamma	0 deg	0.023 deg	0 deg	0 deg
Initial AOB	90 deg	90 deg	86.1 deg	44.3 deg
Inclination change	0.767 deg	0.688 deg	0.681 deg	0.825 deg
Mass Fraction used	2%	2%	2%	2%
Change in Altitude	-61 m	0 m	0 m	0 m
Time required	19.3 sec	19.3 sec	19.3 sec	346 sec
fuel/degree inclination	127.77 kg/deg	142.44 kg/deg	143.91 kg/deg	118.79 kg/deg
% difference over Aerocruise	-7.56 %	-19.91 %	-21.15 %	0 %
	K= 1.02 HEATING RATE		**1.42*10^6 WATTS/M^2**	
	AEROBANG	AEROBANG	AEROBANG	AEROCRUISE
Initial Gamma	0 deg	0.029 deg	0 deg	0 deg
Initial AOB	90 deg	90 deg	85 deg	26.4 deg
Inclination change	0.794 deg	0.694 deg	0.69 deg	0.542 deg
Mass Fraction used	2%	2%	2%	2%
Change in Altitude	-78 m	-1 m	1 m	0 m
Time required	19.3 sec	19.3 sec	19.3 sec	338.8 sec
fuel/degree inclination	123.43 kg/deg	141.21 kg/deg	142.03 kg/deg	180.81 kg/deg
% difference over Aerocruise	31.74 %	21.90 %	21.45 %	0 %

Figure 27 shows the break even point for the efficiency comparison of aerobang to aerocruise to be at approximately k=1.0175; slower than this speed the aerobang method is more efficient in providing an inclination change. At k=1.02, the difference in fuel of the aerobang method over the aerocruise method exceeds 20 percent. This high difference is attributed to the excessive angle of bank required by the aerocruise maneuver to maintain the flight profile.

The aerocruise maneuver for this flight condition is at an angle of bank of 26 degrees, allowing a large portion of the lift to be directed away from the orbit normal and unable to effect the inclination change.

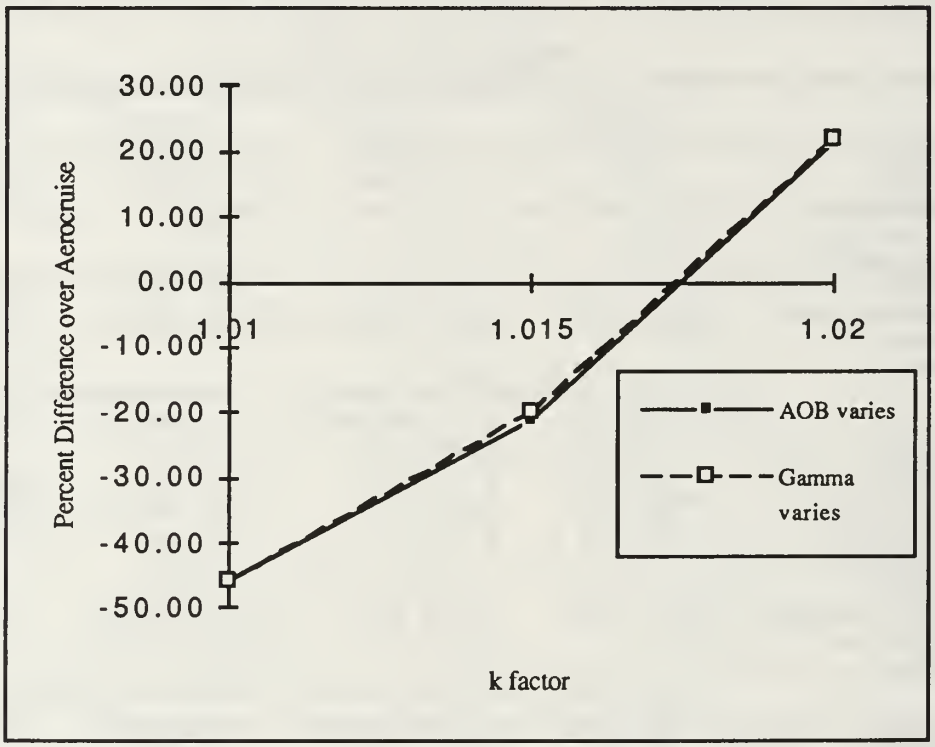

Figure 27. Fuel Percentage Difference over Aerocruise vs k Factor for MRRV (High Heating Rate)

2. Low Heating Rate

a. ERV

The range of flight velocities over which the aerocruise maneuver could operate was narrower from those of the high heating rate. Speeds slower than k=1.05 required an unattainable angle of attack for the aerocruise maneuver. Table 7 summarizes the data gathered for the given set of flight conditions. Comparing the values of specific inclination change (ie, fuel/degree inclination) the two aerobang augmented methods were nearly identical. A

TABLE 7. SUMMARY OF ERV FLIGHT PROFILES FOR LOW HEATING RATE

	K= 1.02 HEATING RATE .9088*10^6 WATTS/M^2							
	AEROBANG		AEROBANG		AEROBANG		AEROCRUISE	
Initial Gamma	0	deg	0.057	deg	0	deg	0	deg
Initial AOB	90	deg	90	deg	84.5	deg	65.3	deg
Inclination change	1.675	deg	1.303	deg	1.3	deg	1.603	deg
Mass Fraction used	4%		4%		4%		4%	
Change in Altitude	-358	m	-6	m	3	m	0	m
Time required	40.9	sec	40.9	sec	40.9	sec	239.1	sec
fuel/degree inclination	124.2	kg/deg	159.6	kg/deg	160	kg/deg	129.8	kg/deg
% difference over Aerocruise	4.31	%	-22.96	%	-23.27	%	0.00	%
	K= 1.03 HEATING RATE .9088*10^6 WATTS/M^2							
	AEROBANG		AEROBANG		AEROBANG		AEROCRUISE	
Initial Gamma	0	deg	0.044	deg	0	deg	0	deg
Initial AOB	90	deg	90	deg	82.2	deg	45.3	deg
Inclination change	0.788	deg	0.655	deg	0.653	deg	0.635	deg
Mass Fraction used	2%		2%		2%		2%	
Change in Altitude	-124	m	0	m	-1	m	0	m
Time required	20.5	sec	20.5	sec	20.5	sec	140.9	sec
fuel/degree inclination	131.98	kg/deg	158.78	kg/deg	159.26	kg/deg	163.78	kg/deg
% difference over Aerocruise	19.42	%	3.05	%	2.76	%	0	%
	K= 1.04 HEATING RATE .9088*10^6 WATTS/M^2							
	AEROBANG		AEROBANG		AEROBANG		AEROCRUISE	
Initial Gamma	0	deg	0.057	deg	0	deg	0	deg
Initial AOB	90	deg	90	deg	79.8	deg	28.9	deg
Inclination change	0.836	deg	0.665	deg	0.658	deg	0.446	deg
Mass Fraction used	2%		2%		2%		2%	
Change in Altitude	-160	m	-2	m	1	m	0	m
Time required	20.5	sec	20.5	sec	20.5	sec	135.2	sec
fuel/degree inclination	124.40	kg/deg	156.39	kg/deg	158.05	kg/deg	233.18	kg/deg
% difference over Aerocruise	46.65	%	32.93	%	32.22	%	0	%
	K= 1.05 HEATING RATE .9088*10^6 WATTS/M^2							
	AEROBANG		AEROBANG		AEROBANG		AEROCRUISE	
Initial Gamma	0	deg	0.069	deg	0	deg	0	deg
Initial AOB	90	deg	90	deg	78	deg	3.7	deg
Inclination change	0.873	deg	0.668	deg	0.661	deg	0.135	deg
Mass Fraction used	2%		2%		2%		2%	
Change in Altitude	-189	m	0	m	1	m	0	m
Time required	20.5	sec	20.5	sec	20.5	sec	130.8	sec
fuel/degree inclination	119.13	kg/deg	155.69	kg/deg	157.34	kg/deg	770.37	kg/deg
% difference over Aerocruise	84.54	%	79.79	%	79.58	%	0	%

demonstrated disadvantage of the flight path angle method of augmentation is that the angle of attack for each simulation exceeded 40 degrees, beyond the flight vehicle's operating envelope. This excessive angle of attack did not occur for any of the angle of bank augmented simulations and while the angle of attack

was high it did not exceed the threshold of the model. Additionally, from Figure 28 it is observed that the aerobang maneuver is more efficient at k=1.03 or greater. Once again the aerobang maneuver has a higher specific inclination change compared to the aerocruise maneuver as the velocity differs more from the circular orbital speed. The time for the two methods to complete the flight profile differed greatly: the aerobang method once again was much faster than the aerocruise method, completing the maneuver approximately 6.5 times faster. For short duration atmospheric interactions, a time differential of this nature may not play an important roll, however, if the atmospheric interactions were of

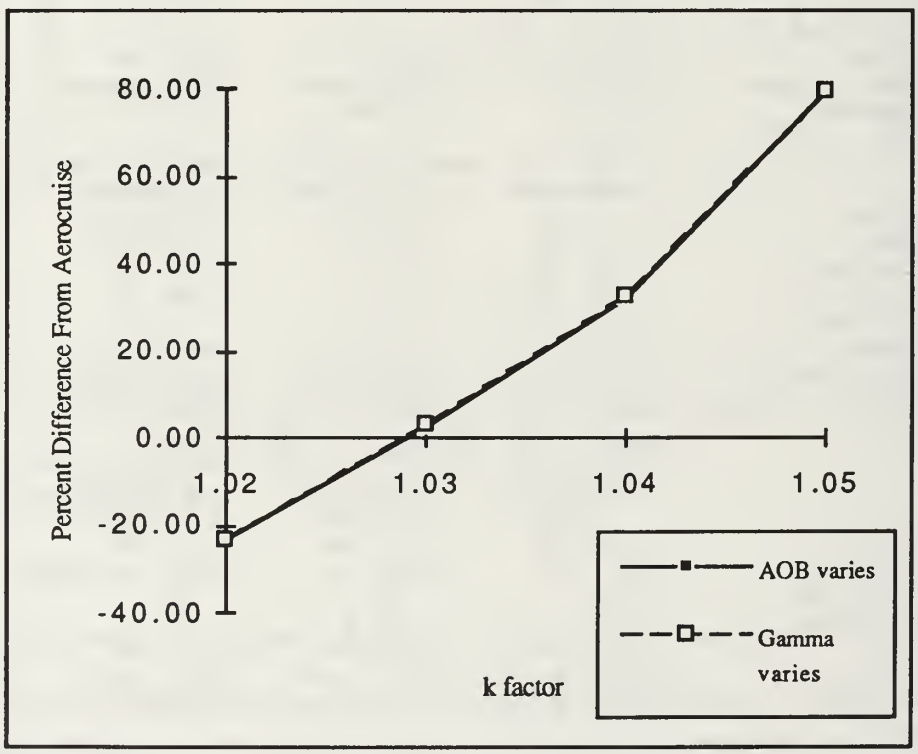

Figure 28. Fuel Percentage Difference over Aerocruise vs k Factor for MRRV (Low Heating Rate)

longer duration, the aerocruise maneuver may approach or exceed a quarter period of its orbit, in which case the inclination change caused by any force in the orbit normal direction is reduced.

b. MRRV

The last set of simulations discussed will be that of the MRRV at a low heating rate value. The MRRV range of flight speeds are very narrow at this heating rate: from k=1.002 to k=1.007. The aerocruise maneuver cannot be performed at speeds slower than this. As previously stated, the narrow range of

TABLE 8. SUMMARY OF MRRV FLIGHT PROFILES FOR LOW HEATING RATE

	K= 1.002 HEATING RATE		.9088*10^6 WATTS/M^2	
	AEROBANG	AEROBANG	AEROBANG	AEROCRUISE
Initial Gamma	0 deg	0.006 deg	0 deg	0 deg
Initial AOB	90 deg	90 deg	89 deg	62.5 deg
Inclination change	0.637 deg	0.619 deg	0.621 deg	0.984 deg
Mass Fraction used	2%	2%	2%	2%
Change in Altitude	-15 m	0 m	-1 m	0 m
Time required	19.3 sec	19.3 sec	19.3 sec	891 sec
fuel/degree inclination	1.09 kg/deg	158.32 kg/deg	157.81 kg/deg	99.59 kg/deg
% difference over Aerocruise	80.62 %	-58.97 %	-58.45 %	0.00 %
	K= 1.005 HEATING RATE		**.9088*10^6 WATTS/M^2**	
	AEROBANG	AEROBANG	AEROBANG	AEROCRUISE
Initial Gamma	0 deg	0.009 deg	0 deg	0 deg
Initial AOB	90 deg	90 deg	88.2 deg	39.3 deg
Inclination change	0.651 deg	0.625 deg	0.623 deg	0.714 deg
Mass Fraction used	2%	2%	2%	2%
Change in Altitude	-26 m	-1 m	0 m	0 m
Time required	19.3 sec	19.3 sec	19.3 sec	879.6 sec
fuel/degree inclination	1.09 kg/deg	156.80 kg/deg	157.30 kg/deg	137.25 kg/deg
% difference over Aerocruise	85.94 %	-14.24 %	-14.61 %	0 %
	K= 1.007 HEATING RATE		**.9088*10^6 WATTS/M^2**	
	AEROBANG	AEROBANG	AEROBANG	AEROCRUISE
Initial Gamma	0 deg	0.013 deg	0 deg	0 deg
Initial AOB	90 deg	90 deg	67.7 deg	12.8 deg
Inclination change	0.661 deg	0.623 deg	0.623 deg	0.29 deg
Mass Fraction used	2%	2%	2%	2%
Change in Altitude	-34 m	0 m	0 m	0 m
Time required	19.3 sec	19.3 sec	19.3 sec	872.2 sec
fuel/degree inclination	1.09 kg/deg	157.30 kg/deg	157.30 kg/deg	337.93 kg/deg
% difference over Aerocruise	94.29 %	53.45 %	53.45 %	0 %

speeds is attributed to the fact that the MRRV was designed to operate aerodynamically at lower altitudes and higher heating rates than the value used. For comparison to the ERV, the range is adequate. Table 8 is the summary of each set of data and Figure 29 graphically represents the data contained in the table. From Figure 29 the aerobang method of inclination change becomes more efficient at speeds slower than k=1.0055. The aerocruise maneuver required nearly 900 seconds to be completed as compared to the 19 seconds for the aerobang maneuver. At 900 seconds the aerocruise maneuver approaches a

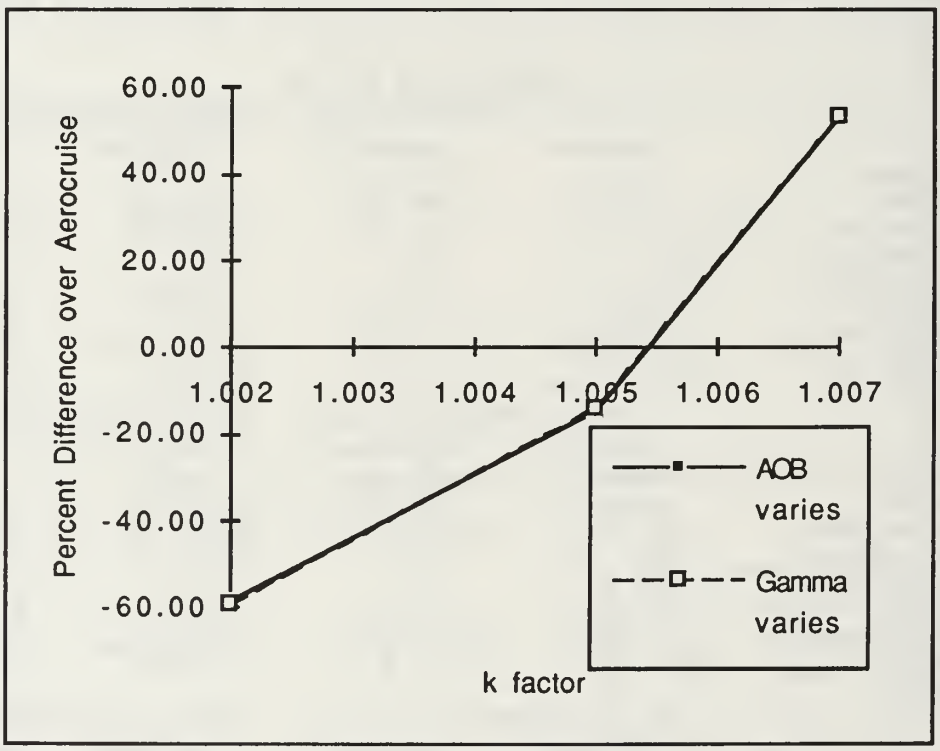

Figure 29. Fuel Percentage Difference over Aerocruise vs k Factor for MRRV (Low Heating Rate)

quarter of an orbital period, beyond the 900 seconds shown, the inclination change per kilogram of fuel falls off to become zero at the apex of the orbit. For this maneuver, the flight vehicle would need to roll over to bring the lift vector to the other side of the orbit or be subject to a decreasing inclination.

D. MASS FRACTION EFFECTS

All of the above analysis was done for fuel expenditure of 2% of spacecraft mass fraction. Because larger inclination changes may be desired, an analysis was done on the possible advantages of expending more than 2% mass fraction of fuel. The effect of longer atmospheric interactions may cause the maneuver to approach the apex of the orbit and decrease the inclination change. The aerobang method is faster at completing the desired inclination change as compared to the aerocruise method. A conclusion can be drawn that the aerobang method should become increasingly better than the aerocruise method as the mass fraction increases. Table 9 shows the effect of increasing mass fraction for the ERV with a flight profile of k=1.03 and a high heating rate. Both methods of altitude maintenance were used and compared to the aerocruise method. The flight path angle method was terminated beyond a mass fraction of 4% because the vehicle could not be flown at the constant heating rate. The angle of bank method of altitude maintenance worked throughout the full range of mass fraction. Figure 30 shows the percentage difference over aerocruise vs the mass fraction. The graph indicates that initially the mass fraction has little effect on the percentage difference over the aerocruise model. As more mass fraction is burned, the effect was as expected; the aerocruise method lost some of its advantage because it approaches the apex of the orbit. For this particular flight profile, the aerocruise maneuver took approximately three times longer

than the aerobang maneuver. For flight profiles which have a higher ratio of maneuver times, the mass fraction advantage effect would occur at lower mass fractions than for the case presented.

TABLE 9. EFFECT OF MASS FRACTION ON INCLINATION CHANGE EFFICIENCY

	K= 1.03 HEATING RATE 1.42*10^6 WATTS/M^2			
	AEROBANG	AEROBANG	AEROBANG	AEROCRUISE
Initial Gamma	0 deg	0.046 deg	0 deg	0 deg
Initial AOB	90 deg	90 deg	83.4 deg	73.3 deg
Inclination change	0.93 deg	0.754 deg	0.765 deg	0.849 deg
Mass Fraction used	2%	2%	2%	2%
Change in Altitude	-124 m	4 m	-2 m	0 m
Time required	20.5 sec	20.5 sec	20.5 sec	57.9 sec
fuel/degree inclination	111.83 kg/deg	137.93 kg/deg	135.95 kg/deg	122.5 kg/deg
% difference over Aerocruise	8.71 %	-12.60 %	-10.98 %	0 %
	K= 1.03 HEATING RATE 1.42*10^6 WATTS/M^2			
	AEROBANG	AEROBANG	AEROBANG	AEROCRUISE
Initial Gamma	0 deg	0.08 deg	0 deg	0 deg
Initial AOB	90 deg	90 deg	83.4 deg	73.3 deg
Inclination change	2.193 deg	1.547 deg	1.546 deg	1.716 deg
Mass Fraction used	4%	4%	4%	4%
Change in Altitude	-516 m	-29 m	-6 m	0 m
Time required	40.9 sec	40.9 sec	40.9 sec	115.7 sec
fuel/degree inclination	94.8 kg/deg	134.45 kg/deg	134.36 kg/deg	121.2 kg/deg
% difference over Aerocruise	21.78 %	-10.93 %	-10.86 %	0 %
	K= 1.03 HEATING RATE 1.42*10^6 WATTS/M^2			
	AEROBANG	AEROBANG*	AEROBANG	AEROCRUISE
Initial Gamma	0 deg	0.097 deg	0 deg	0 deg
Initial AOB	90 deg	90 deg	83.42 deg	73.3 deg
Inclination change	8.684 deg	5.964 deg	3.945 deg	4.412 deg
Mass Fraction used	10%	10%	10%	10%
Change in Altitude	-4092 m	-1760 m	4 m	0 m
Time required	102 sec	102 sec	102 sec	288.5 sec
fuel/degree inclination	59.65 kg/deg	86.85 kg/deg	131.3 kg/deg	117.5 kg/deg
% difference over Aerocruise	49.23 %	26.09 %	-11.74 %	0 %
	K= 1.03 HEATING RATE 1.42*10^6 WATTS/M^2			
	AEROBANG*	AEROBANG*	AEROBANG	AEROCRUISE
Initial Gamma	deg	deg	0 deg	0 deg
Initial AOB	deg	deg	83.77 deg	73.3 deg
Inclination change	deg	deg	19.29 deg	20.095 deg
Mass Fraction used			40%	40%
Change in Altitude	m	m	0 m	0 m
Time required	sec	sec	408.2 sec	1153.8 sec
fuel/degree inclination	kg/deg	kg/deg	107.5 kg/deg	103.2 kg/deg
% difference over Aerocruise	%	%	-4.17 %	0 %

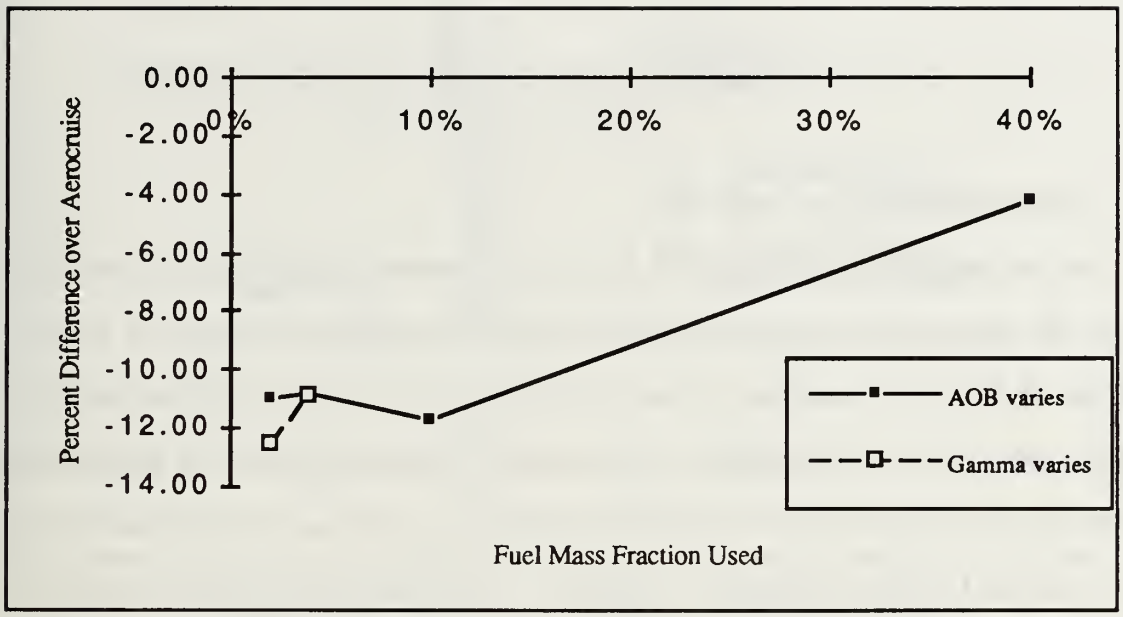

Figure 30. Fuel Percentage Difference over Aerocruise vs Mass Fraction Fuel Expended for ERV (k=1.03)

VII. CONCLUSIONS AND RECOMMENDATIONS

1. CONCLUSIONS

As demonstrated in Chapter VI, there exists a small range of flight speeds in which the aerocruise maneuver exhibits a greater inclination change for a given amount of fuel than does the aerobang maneuver. This range of flight speeds is always centered around circular orbital speed. Figures 31 and 32 graphically shows the flight range where (within the hash marks), the aerocruise maneuver is predicted to be more efficient. However, use of the aerobang maneuver is predicted to be more efficient as the speeds become either more super- or more subcircular (regions beyond the hash marks). These regions of superior aerocruise efficiency, while bracketing the circular orbit speed are not symmetric in nature and tend to be narrower in the supercircular flight regime.

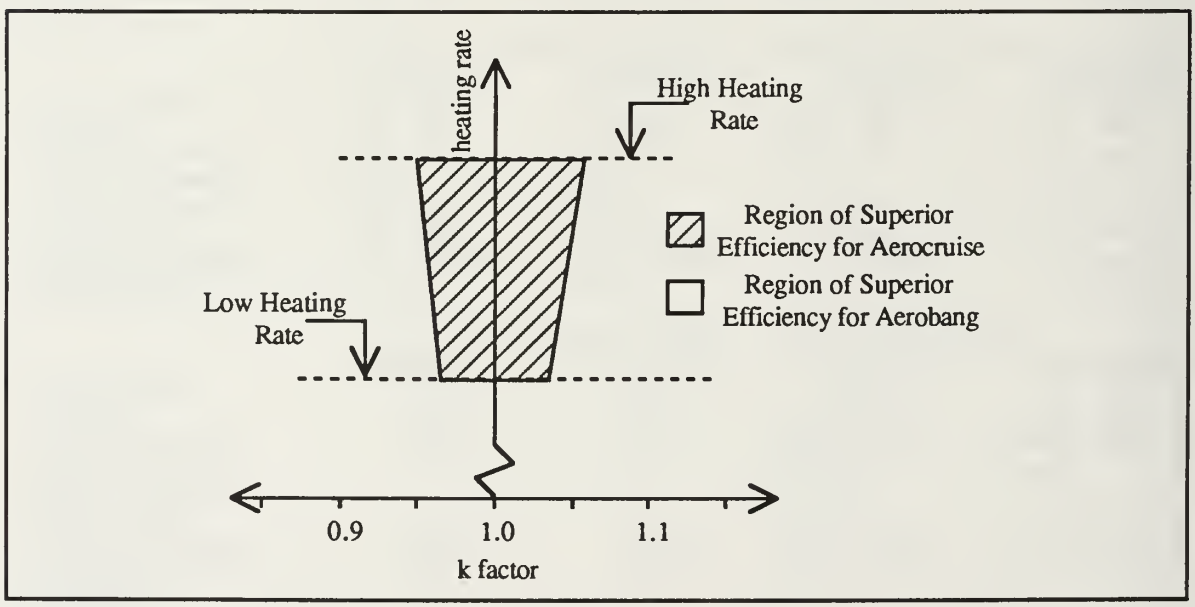

Figure 31. Efficiency Regions for the ERV

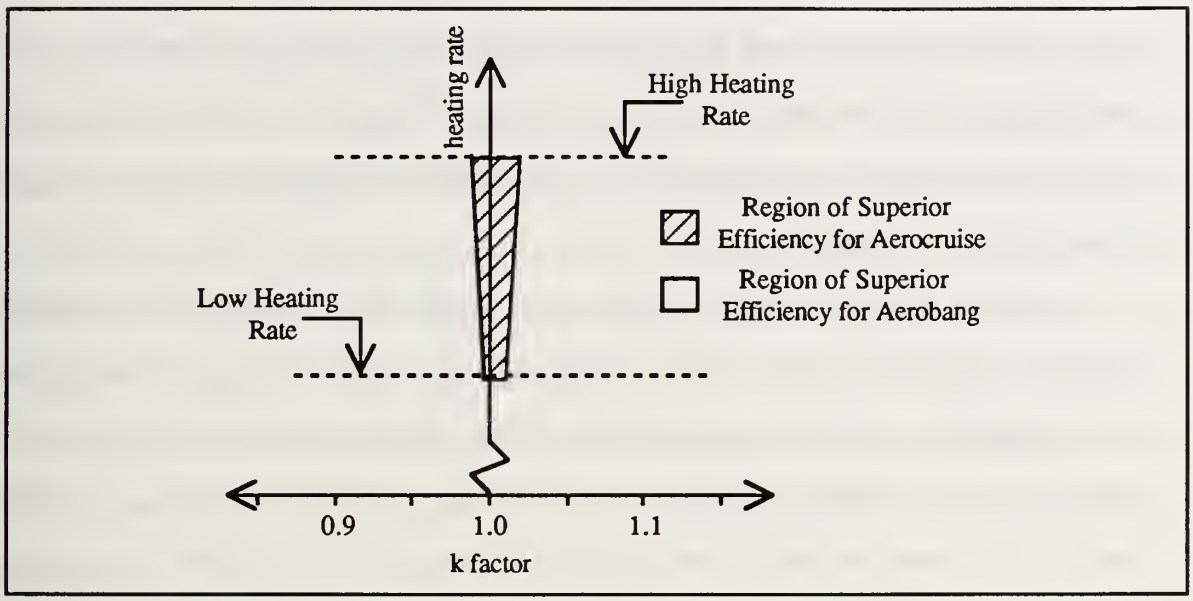

Figure 32. Efficiency Regions for the MRRV

As discussed in Chapter IV, Section A, the aerocruise maneuver was unable to maintain the desired profile at speeds just possible the region of superior efficiency. This result was expected and shows that the the aerobang maneuver has a greater range of operating flight speeds as compared to the aerocruise maneuver.

A higher maneuver efficiency exists for a vehicle with a greater maximum lift-to-drag ratio while executing an aerobang maneuver. The data from the ERV and the MRRV were compared for similar flight profiles, for the case k=1.03 and $\dot{Q} = 1.42*10\text{^}6$ W/m^2. In order to analyze the effect of the lift-to-drag ratio on the inclination change, the effects from factors not associated with the lift-to-drag ratio must be eliminated. A major component which directly influences the amount of inclination change achieved is the lifting force generated by the flight vehicle during the maneuver. Lift generated by the flight vehicle is the product of the dynamic pressure on the vehicle, the coefficient of lift, and the reference wing area. By operating the two vehicles at the same

heating rate and flight speed, the dynamic pressure remains the same for the two simulations. The reference wing area of the ERV and the MRRV differ and must be taken into account in order to isolate the effect the lift-to-drag ratio has on the inclination change.

A scaling factor equivalent to the ratio of the wing areas of ERV and the MRRV is introduced. This scaling factor is used to account for the inclination change lost due to the lower wing area of the MRRV. From Chapter III, the wing area of the MRRV is 28% lower than that of the ERV, yielding a scaling factor of 1.4. Prior to scaling, the inclination change for the MRRV under these flight conditions is 0.693 degrees for a 2% fuel consumption. The ERV attained an inclination change of 0.765 degrees under identical flight conditions. Scaling the MRRV inclination change with the 1.4 factor yields an inclination change of 0.970 degrees, clearly higher than that for the ERV.

As can be seen in Figure 32 the aerocruise-superior flight speed range of operations for the MRRV dramatically narrowed; this may be attributed to the the decreased lift force generated by the smaller coefficient of lift rather than the higher lift-to-drag ratio of the MRRV. The time of flight for the aerobang maneuver was unaffected by the change in the lift-to-drag ratio while for the aerocruise maneuver, the time required to burn a 2% mass fraction of fuel increased for the MRRV. This result was not unexpected because the reduced drag coefficient of the higher lift-to-drag ratio vehicle is reflected in the thrust required to maintain altitude.

Operating at a subcircular speed, the aerobang maneuver would normally results in a loss of altitude. In order to compare this maneuver with the aerocruise maneuver, which loses no altitude, two methods of altitude control

were used (Section VI.A). Of the two methods of altitude maintenance, augmentation of the angle of bank proved to be superior to modification of the initial flight path angle. While there was generally little difference in efficiency from using either method, Figure 24 clearly shows the angle of bank method to be more efficient than the flight path angle method. Additionally, the useful range of operation of the flight path angle method is much smaller than that of the angle of bank method. In all subcircular cases, there existed speeds too low for the flight path angle method to maintain a flight profile at a constant heating rate.

From a fuel efficiency point of view, the percentage difference in fuel burned per unit angle of inclination change between the aerobang and aerocruise methods remains unaltered until the time required to complete the maneuver approaches a quarter of an orbital period for the aerocruise maneuver. This means that a low drag environment (drag force << maximum thrust), the aerobang maneuver will perform better than the aerocruise as more fuel is expended. The reason for this is that the thrust for the aerobang maneuver is not dependent on the drag environment, while the thrust for the aerocruise maneuver is modulated to counteract the drag.

2. FOLLOW ON TOPICS

Simply put, during the maneuver, the aerobang method modulates the angle of attack and the aerocruise method modulates the angle of bank. As shown within this thesis, there exist regions where one method claims superiority over the other. Following this line of thinking, a method of control which modulates both the angle of attack and the angle of bank to realize the best of each maneuver may be of greater efficiency than either of the two methods studied

here. This would require more sophisticated control laws than those discussed above.

Another topic of interest would be to determine whether to use the angle of bank method of maintaining altitude during an aerobang maneuver, or to accept the energy loss normally associated with the subcircular aerobang maneuver and reestablish the orbit with an additional burn after exiting the atmosphere. It may take less fuel to accept the altitude loss from a true aerobang maneuver than to augment the maneuver in order to maintain a specified altitude.

Comparison of the aerocruise data for two flight vehicles operating at similar flight conditions produced a curious result. It is well established that a vehicle with the higher lift-to-drag ratio produces the more efficient maneuver, this was not observed for the aerocruise maneuver and further investigation is warranted. This may perhaps be attributed to the fact that although the aerocruise maneuver operates at the maximum lift-to-drag ratio for the vehicle, the actual values of the drag and lift may be low. If the lift force is low, then the plane-change achieved will also be low for a given arc length regardless of the maximum lift-to-drag ratio.

Finally, there is reason to investigate the unsymmetric nature of the aerocruise-superior region of operations (Figure 32). For both flight vehicles, the supercircular region of the aerocruise-superior area is narrower than the subcircular region. The flight regime where the aerocruise maneuver is superior was expected to center around the circular orbital speed, but in a symmetric nature. The reason why this occurred is unclear at this time and should be addressed in a follow-on study.

APPENDIX A

```
C
      PROGRAM ORBIT
      IMPLICIT REAL*8(A-H,L-Z)
      DIMENSION X(6),XDOT(6),C(6)
      CHARACTER*10 CSE
C
C     PROGRAMMER        : THOMAS P. SPRIESTERBACH
C     DATE              : 15 AUG 91
C     SYSTEM            : VAX/FORTRAN
C
C
C                              VARIABLE LIST
C
C     I           COUNTING INDEX
C     INDEX       COUNTING INDEX FOR RUNGE-KUTTA ROUTINE
C     J           COUNTING INDEX
C     KOUNT       COUNTING INDEX FOR OUTPUT DETERMINATION
C     DUM         DUMMY VARIABLE FOR CONVENIENCE
C     OLDCO       CONTROL VARIABLE FOR CONVERGENCE ON AOA
C     CHANGE      INCREMENTAL CHANGE IN AOA USING NEWTONS METHOD
C     NE          NUMBER OF EQUATIONS OF MOTION
C     CSE         CASE EITHER AEROCRUISE OR AEROBANG
C     T           TIME                                          (SEC)
C     TF          FINAL TIME                                    (SEC)
C     H           INCREMENT OF TIME [RUNGE-KUTTA ROUTINE](SEC)
C     TPI         TIME PRINT INTERVAL                           (SEC)
C     X(1)        RADIUS                                        (METERS)
C     X(2)        THETA                                         (RADIANS)
C     X(3)        PHI                                           (RADIANS)
C     X(4)        VELOCITY                                      (M/S)
C     X(5)        FLIGHT PATH ANGLE GAMMA                       (RADIANS)
C     X(6)        PSI                                           (RADIANS)
C     XDOT()      DERIVATIVES OF THE ABOVE SIX VARIABLES
C     C(1)        ZEROTH ORDER COEFFICIENT FOR CL EQUATION
C     C(2)        FIRST ORDER COEFFICIENT FOR CL EQUATION
C     C(3)        SECOND ORDER COEFFICIENT FOR CL EQUATION
C     C(4)        ZEROTH ORDER COEFFICIENT FOR CD EQUATION
C     C(5)        FIRST ORDER COEFFICIENT FOR CD EQUATION
C     C(6)        SECOND ORDER COEFFICIENT FOR CD EQUATION
C     BETA        DENSITY MODEL EXPONENT                        (METERS)
C     G0          GRAVITY AT EARTH SURFACE                      (9.806 M^2/S)
C     G           LOCAL GRAVITATIONAL ATTRACTION                (M^2/S)
C     H0          REFERENCE ALTITUDE FOR DENSITY MODEL          (METERS)
C     RHO0        REFERENCE DENSITY FOR DENSITY MODEL           (KG/M^3)
C     MU          GRAVITATIONAL CONSTANT
C     ALPHA       ANGLE OF ATTACK                               (RADIANS)
```

```
C   ALFA        ANGLE OF ATTACK                                  (DEG)
C   AOPT        ANGLE OF ATTACK AT MAX CL/CD                     (RADIANS)
C   MASS        MASS OF SPACECRAFT                               (KG)
C   MASS0       INITIAL MASS OF SPACECRAFT                       (KG)
C   SPI         SPECIFIC IMPULSE OF POWER PLANT                  (SEC)
C   R           RADIUS                                           (M)
C   V           VELOCITY                                         (M/S)
C   RADIUS      RADIUS                                           (KM)
C   VELOCITY    VELOCITY                                         (KM/S)
C   GAMMA       FLIGHT PATH ANGLE                                (DEG)
C   ANGM        ANGULAR MOMENTUM                                 (M^2/S)
C   SIGMA       ANGLE OF BANK                                    (DEG)
C   OINC        INCLINATION                                      (DEG)
C   DELTA       INTERMEDIATE ANGLE                               (DEG)
C   OMEGA       LONGITUDE OF THE ASCENDING NODE                  (DEG)
C   AS          TANGENTIAL ACCELERATION                          (M/S^2)
C   AR          RADIAL ACCELERATION                              (M/S^2)
C   AW          BINORMAL ACCELERATION                            (M/S^2)
C   THR         THRUST                                           (N)
C   AOB         ANGLE OF BANK                                    (RADIANS)
C   RHO         DENSITY                                          (KG/M^3)
C   S           REFERENCE AREA OF SPACECRAFT                     (M^2)
C   N           DENSITY COEFFICIENT FOR HEATING RATE EQUATION
C   M           VELOCITY COEFFICIENT FOR HEATING RATE EQUATION
C   HEAT        STAGNATION POINT HEATING RATE                    (WATTS/M^2)
C   QS          DYNAMIC PRESSURE TIMES THE REF AREA              (N*M^2)
C   CD          COEFFICIENT OF DRAG
C   CL          COEFFICIENT OF LIFT
C   LIFT        LIFT ON SPACECRAFT                               (N)
C   DRAG        DRAG ON SPACECRAFT                               (N)
C
CCCCCCCCCCCCCCCCCCCCCCCCCCCCCCCCCCCCCCCCCCCCCCCCCCCCCCCCCCCCCCCCCCCCCC
C
C    DEFINED FUNCTION FOR ACCEL DUE TO GRAVITY
C
      G(R)=MU/(R*R)
C
CCCCCCCCCCCCCCCCCCCCCCCCCCCCCCCCCCCCCCCCCCCCCCCCCCCCCCCCCCCCCCCCCCCCCC
C
C    OPEN TWO INPUT FILES.....DATA.DAT   -  ORBITAL PARMS
C                             AERO.DAT   -  VEHICLE PARMS
C       ONE INPUT FILE.....OUT.DAT    -  TABLE OF VALUES
C
CCCCCCCCCCCCCCCCCCCCCCCCCCCCCCCCCCCCCCCCCCCCCCCCCCCCCCCCCCCCCCCCCCCCCC
C
      OPEN(10,FILE='DATA',STATUS='OLD')
      OPEN(12,FILE='AERO',STATUS='OLD')
      OPEN(13,FILE='OUT',STATUS='NEW')

      READ(10,1)CSE,(X(I),I=1,6),T,TF,H,TPI
1     FORMAT(/,/,20X,A10,10(/,20X,D13.7))
```

```
      READ(12,2)(C(I),I=1,6),AOPT,AOB,N,M,S,MASS0,FM,SPI,THR
2     FORMAT(/,/,/,/,15(/,20X,D13.7))

CCCCCCCCCCCCCCCCCCCCCCCCCCCCCCCCCCCCCCCCCCCCCCCCCCCCCCCCCCCCCCCCCCC
C
C     PRINT CASE TO SCREEN FOR VISUAL VERIFICATION OF SELECTION
C
CCCCCCCCCCCCCCCCCCCCCCCCCCCCCCCCCCCCCCCCCCCCCCCCCCCCCCCCCCCCCCCCCCC
      WRITE(6,*)CSE,'*'
      WRITE(6,*)
C
C     NUMBER OF EQUATIONS TO INTEGRATE
C      X(1)....RADIUS
C     X(2)....THETA (SPHERICAL COORD. PARAMETER)
C     X(3)....PHI   (SPHERICAL COORD. PARAMETER)
C     X(4)....VELOCITY
C     X(5)....FLIGHT PATH ANGLE GAMMA
C      X(6)....PSI
C
C     INITIALIZATION OF CONSTANTS
C
      NE=6
      PI=3.14159265359D+0
      MU=3.986012D+14
      G0=9.806D+0
      MASS=MASS0
C
C     MAIN PROGRAM
C
      INDEX=0
      KOUNT=1
C
C     INITIAL CALL TO GET ACCELERATIONS AND CONTROL VARIABLES
C     FOR FIRST OUTPUT
C
      CALL CNTRL(DRAG,LIFT,THR,ALPHA,AOB,X,MASS,S,C,N,M,
     *RHO,CSE,AOPT)
      CALL ACEL(AS,AR,AW,DRAG,LIFT,THR,ALPHA,AOB,MASS)

      CALL HDR(X(1),X(4),MASS,THR,X(5),CSE)
      CALL WRT(X,T,THR,MASS,ALPHA,AOB,RHO,N,M)

CCCCCCCCCCCCCCCCCCCCCCCCCCCCCCCCCCCCCCCCCCCCCCCCCCCCCCCCCCCCCCCCCCC
C     THIS IS THE MAIN BLOCK OF THE PROGRAM CALLING FIRST THE
C     CONTROL SUBROUTINE TO DETERMINE THE CONTROL METHOD AND
C     OUTPUT VARIABLES.  NEXT ON TO THE ACCELERATION ROUTINE TO
C     CALCULATE THE RELATIVE ACCELERATION TO THE VEHICLE, THEN ON
C     TO THE DIFFERENTIAL EQUATIONS OF MOTION AND FINALLY A
C     FOURTH ORDER RUNGE-KUTTA ROUTINE.  THIS BLOCK IS COMPUTED
C     AT EACH TIME INCREMENT H.
```

```
C
CCCCCCCCCCCCCCCCCCCCCCCCCCCCCCCCCCCCCCCCCCCCCCCCCCCCCCCCCCCCCCCC
100   CALL CNTRL(DRAG,LIFT,THR,ALPHA,AOB,X,MASS,S,C,N,M,
     *RHO,CSE,AOPT)
      CALL ACEL(AS,AR,AW,DRAG,LIFT,THR,ALPHA,AOB,MASS)
      CALL ORB(X,XDOT,AS,AR,AW,G(X(1)))
      CALL RK4(T,X,XDOT,NE,H,INDEX)
      IF(INDEX .NE. 0) GO TO 100

C     DETERMINE IF TIME TO PRINT TO OUTPUT USING TIME PRINT
C     INTERVAL

200   IF(KOUNT .LT. IDNINT(TPI/H)) GO TO 300

      CALL WRT(X,T,THR,MASS,ALPHA,AOB,RHO,N,M)

C     PRINT STATUS TO TERMINAL

      WRITE(6,7)T,ALPHA,AOB
7     FORMAT('+',F8.1,1X,F6.3,1X,F6.3)

      KOUNT=0
300   KOUNT=KOUNT+1
C
C     CHANGE MASS OF S/C
C
      MASS=MASS-THR*H/(SPI*G0)
C
C     TWO TESTS EITHER CAN STOP THE PROGRAM. TEST FOR MASS LESS
C     THAN FINAL MASS AND ALSO IF TIME IS GREATER THAN FINAL TIME
C
      IF(MASS .GT. FM .AND. T .LE. TF) GO TO 100
C
C     PRINT OUTPUT AGAIN IF MASS SWITCH ENDED PROGRAM
C
      IF(MASS .LE. FM) CALL WRT(X,T,THR,MASS,ALPHA,AOB,RHO,N,M)
C
      END
CCCCCCCCCCCCCCCCCCCCCCCCCCCCCCCCCCCCCCCCCCCCCCCCCCCCCCCCCCCCCCCC
C     THIS SUBROUTINE CALCULATES THE CONTROL OF THE FREE
C     VARIABLES DURING THE ATMOSPHERIC PENETRATION
C
CCCCCCCCCCCCCCCCCCCCCCCCCCCCCCCCCCCCCCCCCCCCCCCCCCCCCCCCCCCCCCCC
      SUBROUTINE CNTRL(DRAG,LIFT,THR,ALPHA,AOB,X,MASS,S,C,N,M
     *,RHO,CSE,AOPT)
      IMPLICIT REAL*8(A-H,L-Z)
      CHARACTER*10 CSE
      DIMENSION X(6),C(6)
C
      MU=3.986012D+14
      GAMMA=X(5)
```

```
      R=X(1)
      V=X(4)
C
C     COEFFICIENTS FOR AN EXPONENTIAL DENSITY MODEL
C     REFERENCE J MEASE 1976 US STANDARD ATMOSPHERE
C     RANGE 50KM TO 120KM
C
      BETA=1.41D-4
      RHO0=3.0968D-4
      R0=6.438D+6

      G=MU/(R*R)
      RHO=RHO0*EXP(-BETA*(R-R0))
      QS=.5D+0*RHO*V*V*S

C
C     THE FIRST CASE IS FOR THE AEROBANG CONTROL LAW AND THE
C     SECOND IS FOR THE AEROCRUISE CONTROL LAW.  FOR AEROBANG THE
C     AOB IS SET AND THE ANGLE OF ATTACK IS CONTROLLED TO FLY AT A
C     CONSTANT HEATING RATE, THE ALTITUDE AND VELOCITY ARE
C    ALLOWED TO FLOAT
C
      IF (CSE.EQ.'AEROBANG  ') THEN
C
C     GUESS ALPHA INITIALLY FOR NEWTON APPROXIMATION ROUTINE
C
      ALPHA=(C(5)*QS+SQRT(C(5)**2+4.*QS*C(6)*(THR-QS*C(4))))
     */(2.*C(6)*QS)
C
C     USE NEWTON APPROXIMATION METHOD TO CONVERGE ON ALPHA FOR
C     AEROBANG USE A WHILE STRUCTURE FOR THE CONVERGENCE OF
C     ALPHA SET OLDCO AND CHANGE EQUAL TO THE VALUES BELOW TO
C     ENSURE THAT THE PROGRAM SWITCHES ARE NOT INITIALLY TRIPPED
C
      OLDCO=1.D+10
      CHANGE=1.
C
      DO WHILE (ABS(CHANGE) .GT. 1.D-3)
C
      CL=C(1)+C(2)*ALPHA+C(3)*ALPHA**2
      CD=C(4)+C(5)*ALPHA+C(6)*ALPHA**2
C
      LIFT=CL*QS
      DRAG=CD*QS
C
C     THESE THREE EQUATIONS REPRESENT THE FUNCTION AND ITS
C     DERIVATIVE WITH RESPECT TO ALPHA FOR NEWTON'S METHOD OF
C     APPROXIMATION
C
      COEFF=(THR*COS(ALPHA)-DRAG)-
     *MASS*SIN(GAMMA)*(G+BETA*(N/M)*V*V)
```

```
      COEFP=-THR*SIN(ALPHA)-(C(5)+2*C(6)*ABS(ALPHA))*QS
C
      CHANGE=COEFF/COEFP

      ALPHA=ALPHA-CHANGE
      IF (ABS(OLDCO)-ABS(CHANGE).LE.0.) STOP
      OLDCO=CHANGE
      END DO
C
      ELSE
C
C     THIS IS THE CONTROL ROUTINE FOR AEROCRUISE. THRUST COUNTER
C     BALANCES THE DRAG AND THE ANGLE OF BANK IS SET TO CONTROL
C     THE ORBIT AT CONSTANT ALTITUDE
C
      ALPHA=AOPT
C
      CL=C(1)+C(2)*ALPHA+C(3)*ALPHA**2
      CD=C(4)+C(5)*ALPHA+C(6)*ALPHA**2
C
      LIFT=CL*QS
      DRAG=CD*QS
C
      THR=DRAG/COS(ALPHA)

C     FORTRAN STOP IF IT IS IMPOSSIBLE TO FLY AN AEROCRUISE PROFILE
C     THIS OCCURS WHEN THE PROGRAM TRIES TO FIND AN AOB IN WHICH
C     THE COSINE OF IT IS GREATER THAN ONE.


      IF(ABS(MASS*(((G*R-V**2)/R)/(THR*SIN(ALPHA)+LIFT))).GT.1.)STOP

      AOB=ACOS(MASS*(((G*R-V**2)/R)/(THR*SIN(ALPHA)+LIFT)))
C
      ENDIF
C
      RETURN
      END
C
CCCCCCCCCCCCCCCCCCCCCCCCCCCCCCCCCCCCCCCCCCCCCCCCCCCCCCCCCCCCCCCCCCCC
C
C     THIS SUBROUTINE DEFINES THE ACCELERATIONS TANGENTIAL,
C     PERPENDICULAR AND RADIAL TO THE ORBITAL PLANE
C
CCCCCCCCCCCCCCCCCCCCCCCCCCCCCCCCCCCCCCCCCCCCCCCCCCCCCCCCCCCCCCCCCCCC
C
      SUBROUTINE ACEL(AS,AR,AW,DRAG,LIFT,THR,ALPHA,AOB,MASS)
      IMPLICIT REAL*8(A-H,L-Z)
C
C     COMPUTE THE ACCELERATIONS ON THE FLIGHT VEHICLE USING
C     EQUATIONS 3.28, 3.29, AND 3.30
```

```
C
      AS=(THR*COS(ALPHA)-DRAG)/MASS
      AW=(LIFT+THR*SIN(ALPHA))*SIN(AOB)/MASS
      AR=(LIFT+THR*SIN(ALPHA))*COS(AOB)/MASS
C
      RETURN
      END
C
CCCCCCCCCCCCCCCCCCCCCCCCCCCCCCCCCCCCCCCCCCCCCCCCCCCCCCCCCCCCCCCCCCC
C
C     THIS SUBROUTINE IS THE COLLECTION OF DIFFERENTIAL EQUATIONS
C     WHICH DESCRIBE THE MOTION OF THE SPACECRAFT EQUATIONS
C      3.9, 3.10, 3.11, 3.31,3.32, AND 3.33
C
CCCCCCCCCCCCCCCCCCCCCCCCCCCCCCCCCCCCCCCCCCCCCCCCCCCCCCCCCCCCCCCCCCC
C
      SUBROUTINE ORB(X,XDOT,AS,AR,AW,G)
      IMPLICIT REAL*8(A-H,L-Z)
      DIMENSION X(6),XDOT(6)
C
      XDOT(1)=X(4)*SIN(X(5))
      XDOT(2)=X(4)*COS(X(5))*COS(X(6))/(X(1)*COS(X(3)))
      XDOT(3)=X(4)*COS(X(5))*SIN(X(6))/X(1)
      XDOT(4)=AS-G*SIN(X(5))
      XDOT(5)=(AR-G*COS(X(5))+X(4)*X(4)*COS(X(5))/X(1))/X(4)
      DUM=TAN(X(3))/X(1)
      XDOT(6)=AW/(COS(X(5))*X(4))-X(4)*COS(X(5))*COS(X(6))*DUM
C
      RETURN
      END
C
CCCCCCCCCCCCCCCCCCCCCCCCCCCCCCCCCCCCCCCCCCCCCCCCCCCCCCCCCCCCCCCCCCC
C
C    THIS SUBROUTINE TAKES CARE OF ALL HARDCOPY OUTPUT
C
CCCCCCCCCCCCCCCCCCCCCCCCCCCCCCCCCCCCCCCCCCCCCCCCCCCCCCCCCCCCCCCCCCC
C
C
      SUBROUTINE WRT(X,T,THR,MASS,ALPHA,AOB,RHO,N,M)
      IMPLICIT REAL*8(A-H,L-Z)
      DIMENSION X(6),XDOT(6)

      PI=3.14159265359D+0

      RADIUS=X(1)/1000.
      VELOCITY=X(4)/1000.
      GAMMA=X(5)*180./PI
      ALFA=ALPHA*180./PI
      HEAT=RHO**N*X(4)**M*9.652D-5
      SIGMA=AOB*180./PI
      OINC=ACOSD(COS(X(3))*COS(X(6)))
```

```
      DELTA=0.0
      IF (OINC .NE. 0.) DELTA=ASIND(TAN(X(3))/TAND(OINC))
      OMEGA=X(2)*180./PI-DELTA

      WRITE(13,1)T,RADIUS,VELOCITY,MASS,GAMMA,OINC,THR,HEAT,ALFA
      ,SIGMA

1     FORMAT(1X,F6.1,1X,F8.3,1X,F6.4,2X,F7.2,1X,F5.3,1X,F6.3,1X,F7.1,
     *1X,E9.3,1X,F7.3,1X,F7.3)
C
      RETURN
      END
C
CCCCCCCCCCCCCCCCCCCCCCCCCCCCCCCCCCCCCCCCCCCCCCCCCCCCCCCCCCCCCCCCCCC
C
C     THIS SUBROUTINE ATTACH A HEADER TO THE OUTPUTS SO I CAN KEEP
C     TRACK OF THE DIFFERENT CHANGES
C
CCCCCCCCCCCCCCCCCCCCCCCCCCCCCCCCCCCCCCCCCCCCCCCCCCCCCCCCCCCCCCCCCCC
C
      SUBROUTINE HDR(R,V,MASS,THR,GAMMA,CSE)
      IMPLICIT REAL*8(A-H,L-Z)
      CHARACTER*10 CSE
      DO 1 I=13,14
      IF (I.EQ.14)GO TO 1
      WRITE(I,*)
      WRITE(I,*)'  SELECTED INITIAL INPUT DATA:'
      WRITE(I,*)
      WRITE(I,2)CSE
      WRITE(I,3)R,V,MASS,THR,GAMMA
      WRITE(I,*)
      WRITE(I,*)
1     CONTINUE
2     FORMAT(1X,A10)
3     FORMAT(' INITIAL RADIUS    (METERS)      ',F10.2,/,' INITIAL
     *VELOCITY  (METERS/SEC)     ',F7.2,/,' INITIAL MASS     (KG)
     *           ',F7.2,/,' INITIAL THRUST    (NEWTONS)      '
     *,F9.2,/,' INITIAL FLIGHT PATH ANGLE (RADS)    ',F7.5)
C
      WRITE(13,*)'  TIME  RADIUS VELOCITY  MASS   GAMMA  INCLI
     *  THRUST   QDOT    ALPHA    AOB'
      WRITE(13,*)' (SEC)   (KM)  (KM/SEC)  (KG)   (DEG)  (DEG)
     *   (N)    (J/M2S)   (DEG)   (DEG)'
C
      RETURN
      END
C
CCCCCCCCCCCCCCCCCCCCCCCCCCCCCCCCCCCCCCCCCCCCCCCCCCCCCCCCCCCCCCCCCCC
C
C     THIS SUBROUTINE IS A FOURTH ORDER RUNGE-KUTTA ROUTINE
C     TAKEN FROM PROF. ROSS SUBROUTINE
```

```
C
CCCCCCCCCCCCCCCCCCCCCCCCCCCCCCCCCCCCCCCCCCCCCCCCCCCCCCCCCCCCCCCC
C
      SUBROUTINE RK4(T,X,XDOT,NE,H,INDEX)
      IMPLICIT REAL*8(A-H,L-Z)
      INTEGER INDEX,I
      DIMENSION X(6),XDOT(6),SAVED(6),SAVEX(6)
C
      INDEX=INDEX+1
      GO TO (1,2,3,4),INDEX
1     DO 10 I=1,NE
      SAVEX(I)=X(I)
      SAVED(I)=XDOT(I)
10    X(I)=SAVEX(I)+.5D0*H*XDOT(I)
      T=T+.5D0*H
      RETURN
C
2     DO 20 I=1,NE
      SAVED(I)=SAVED(I)+2.D0*XDOT(I)
20    X(I)=SAVEX(I)+.5D0*H*XDOT(I)
      RETURN
C
3     DO 30 I=1,NE
      SAVED(I)=SAVED(I)+2.D0*XDOT(I)
30    X(I)=SAVEX(I)+H*XDOT(I)
      T=T+.5D0*H
      RETURN
C
4     DO 40 I=1,NE
40    X(I)=SAVEX(I)+H/6.D0*(SAVED(I)+XDOT(I))
      INDEX=0
      RETURN
      END
```

SAMPLE INPUT DATA FILE "DATA.DAT"

This data file is for the orbital parameters of the chosen flight vehicle The name of the variable is on the left and the value placed on the right using a D13.6 format.

TYPE	AEROBANG
RADIUS METERS	6.4517440D+06
THETA RADIANS	0.0000000D+00
PHI RADIANS	0.0000000D+00
VELOCITY M/S	7.6922000D+03
FLIGHT PATH ANGLE	0.0000000D+00
PSI RADIANS	0.0000000D+00
BEGIN TIME SEC	0.0000000D+00
END TIME SEC	6.0000000D+02
TIME INTERVAL SEC	1.0000000D-02
PRINT TIME INTERVAL	1.0000000D+00

SAMPLE INPUT FILE "AERO.DAT"

This data file is for the aerodynamic parameters of the chosen flight vehicle The name of the variable is on the left and the value placed on the right using a D13.6 format. Coefficients 1-6 are the lift and drag binomial coefficient

COEFFICIENT C1	1.500000D-02
COEFFICIENT C2	9.850000D-01
COEFFICIENT C3	9.240000D-01
COEFFICIENT C4	9.700000D-02
COEFFICIENT C5	-3.340000D-01
COEFFICIENT C6	2.619000D+00
AOA FOR CL/CD MAX	2.440000D-01
AOB FOR BANG MANU	1.570796D+00
DENSITY EXPONENT	0.500000D+00
VELOCITY EXPONENT	3.150000D+00
REFERENCE AREA	1.648000D+01
INITIAL MASS (KG)	5.185000D+03
FINAL MASS (KG)	5.081000D+03
SPECIFIC IMPULSE (S)	2.950000D+02
THRUST (N)	1.469700D+04

SAMPLE OUTPUT FILE "OUT.DAT"

SELECTED INITIAL INPUT DATA:

AEROBANG
INITIAL RADIUS (METERS) 6445000.00
INITIAL VELOCITY (METERS/SEC) 7621.30
INITIAL MASS (KG) 5185.00
INITIAL THRUST (NEWTONS) 14697.00
INITIAL FLIGHT PATH ANGLE (RADS) 0.00170

TIME (SEC)	RADIUS (KM)	VELOCITY (KM/SEC)	MASS (KG)	GAMMA (DEG)	INCLI (DEG)	THRUST (N)	QDOT (J/M2S)	ALPHA (DEG)	AOB (DEG)
0.0	6445.000	7.6213	5185.00	0.097	0.000	14697.0	0.142E+07	3.602	90.000
2.0	6445.025	7.6255	5174.85	0.089	0.022	14697.0	0.142E+07	9.203	90.000
4.0	6445.047	7.6294	5164.69	0.080	0.053	14697.0	0.142E+07	11.580	90.000
6.0	6445.067	7.6328	5154.53	0.072	0.091	14697.0	0.142E+07	13.385	90.000
8.0	6445.085	7.6359	5144.37	0.063	0.135	14697.0	0.142E+07	14.892	90.000
10.0	6445.101	7.6386	5134.20	0.055	0.183	14697.0	0.142E+07	16.207	90.000
12.0	6445.115	7.6409	5124.04	0.047	0.236	14697.0	0.142E+07	17.386	90.000
14.0	6445.126	7.6429	5113.88	0.039	0.292	14697.0	0.142E+07	18.461	90.000
16.0	6445.136	7.6445	5103.72	0.031	0.353	14697.0	0.142E+07	19.454	90.000
18.0	6445.143	7.6457	5093.56	0.023	0.417	14697.0	0.142E+07	20.380	90.000
20.0	6445.148	7.6466	5083.40	0.015	0.484	14697.0	0.142E+07	21.251	90.000
22.0	6445.151	7.6471	5073.24	0.008	0.555	14697.0	0.142E+07	22.074	90.000
24.0	6445.152	7.6473	5063.08	0.000	0.629	14697.0	0.142E+07	22.857	90.000
26.0	6445.151	7.6471	5052.91	-.008	0.706	14697.0	0.142E+07	23.604	90.000
28.0	6445.148	7.6465	5042.75	-.016	0.786	14697.0	0.142E+07	24.321	90.000
30.0	6445.143	7.6456	5032.59	-.024	0.869	14697.0	0.142E+07	25.010	90.000
32.0	6445.135	7.6444	5022.43	-.032	0.955	14697.0	0.142E+07	25.675	90.000
34.0	6445.126	7.6427	5012.27	-.040	1.044	14697.0	0.142E+07	26.318	90.000

LIST OF REFERENCES

1. Sanger, E. and Bredt, I., *A Rocket Drive for Long Range Bombers*, Bureau of Aeronautics, Navy Department, Translation Number CGD-32, 1944.

2. London, Howard S., "Comments on Aerodynamic Plane Change," *AIAA Journal* , v. 1, October 1963.

3. Walberg, Gerald D., "A Survey of Aeroassisted Orbit Transfer," *Journal of Spacecraft and Rocket*, v. 22, January-February 1985.

4. Ross, Michael I., "The GLC and Optimality of the Aerocruise Maneuver," paper presented at the AAS/AIAA Astrodynamics Specialist Conference, Durango, Colorado, 19-22 August 1991.

5. Mease, Kenneth D., Lee, J. Y., and Vinh, N. X., "Orbital Changes during Hypersonic Aerocruise," *The Journal of the Astronautical Sciences*, v. 36, January-February 1988.

6. Ikawa, Hideo and Rudiger, Thomas F., "Synergetic Maneuvering of Winged Spacecraft for Orbital Plane Change," *Journal of Spacecraft and Rocket*, v. 19, November-December 1982.

7. Powel, Richard W., Naftel, Chris J., and Cunningham, Mark J., "Performance Evaluation of an Entry Research Vehicle," *Journal of Spacecraft and Rocket*, v. 24, November-December 1987.

8. Blissit, James A., *An Adaptive Guidance Algorithm for an Aerodynamically Assisted Orbital Plane Change Maneuver*, Master's Thesis, Massachusetts Institute of Technology, Massachusetts, May 1986.

9. Anderson, John D., *Hypersonic and High Temperature Gas Dynamics*, McGraw-Hill Book Company, 1989.

10. Neter, John and Wasserman, William, *Applied Linear Statistical Models*, Richard D. Irwin, 1974.

11. Mease,Kenneth D. and Utashima, Masayoshi, "Effect of Heat Rate Constraint on Minimum-Fuel Synergetic Plane Change," paper presented at the AAS/AIAA Spaceflight Mechanics Meeting, Houston, Texas, 11-13 February 1991.

12. Berkey, Dennis D., *Calculus,* Saunders College Publishing, 1988.

13. Cervisi, Richard T., "Analytic Solution for a Cruising Plane Change Maneuver," *Journal of Spacecraft and Rocket*, v. 22, March-April 1985.

14. Freeman, Delma C., Powel, Richard W., Naftel, Chris J., and Wurster, Kathryn E., "Definition of an Entry Research Vehicle," *Journal of Spacecraft and Rocket*, v. 24, May-June 1987.

INITIAL DISTRIBUTION LIST

		No. Copies
1.	Defense Technical Information Center Cameron Station Alexandria, Virginia 22304-6145	2
2.	Library, Code 0052 Naval Postgraduate School Monterey, California 93943-5002	2
3.	Department Chairman, Code AA Department of Aeronautics and Astronautics Naval Postgraduate School Monterey, California 93943-5000	1
4.	Department of Aeronautics and Astronautics ATTN: Professor I. M. Ross, Code AA/Ro Naval Postgraduate School Monterey, California 93943-5000	7
5.	Department of Aeronautics and Astronautics ATTN: Professor Raymond P. Shreeve, Code AA/Sf Naval Postgraduate School Monterey, California 93943-5000	1
6.	Lieutenant Thomas P. Spriesterbach 1620 Five Forks Rd. Virginia Beach, Virginia 23455	2